Luteolin Restricts Dengue Virus Replication Through Inhibition of the Proprotein Convertase Furin

Minhua Peng[a,b], Satoru Watanabe[b], Kitti Wing Ki Chan[b], Qiuyan He[a], Ya Zhao[a,c], Zhongde Zhang[d], Xiaoping Lai[a], Dahai Luo[e], Subhash G. Vasudevan[b,*] and Geng Li[a,*]

[a]Department of Chinese Medicine, Guangzhou University of Chinese Medicine, Guangzhou 510006, China.

[b]Program in Emerging Infectious Disease, Duke-NUS Medical School, Singapore 169857.

[c]Guangdong Provincial Academy of Chinese Medicine, Guangzhou 510120, China

[d]Emergency Department, Guangdong Provincial Hospital of Chinese Medicine, Guangzhou 510120, China.

[e]Lee Kong Chian School of Medicine, Nanyang Technological University, Singapore 636921.

Corresponding author: Subhash G. Vasudevan, E-mail: subhash.vasudevan@duke-nus.edu.sg; Geng Li, E-mail: lg@gzucm.edu.cn

Abstract

The increasing prevalence of dengue fever in the Indian sub-continent and Southern China is a major public health concern. There is currently an approved tetravalent vaccine available in a handful of countries for protection from dengue infection, but its efficacy against dengue virus (DENV) serotype 2 is not ideal and its overall performance in children under 9 years of age is poor. In many of the dengue afflicted countries-traditional medicine is widely used as a panacea for illnesses and here we describe the systematic evaluation of a natural product, luteolin, originating from the "heat clearing" class of herbs. We show that luteolin is an efficient inhibitor of all four serotypes of DENV and ADE-mediated DENV infection *in vitro* in human cell lines and primary PBMCs respectively. In a time-of-drug-addition study, luteolin was found to reduce infectious virus particle formation but not viral RNA synthesis in Huh-7 cells. Further analysis revealed that secreted uninfectious virus contained precursor membrane (prM) protein that was not cleaved, and biochemical interrogation of human furin showed that luteolin inhibited the enzyme activity in an uncompetitive manner with Ki value of 58.6 μM. Luteolin also exhibited *in vivo* antiviral activity resulting in reduced viremia. Given the mode of action of luteolin and its widespread source it is possible that it can be tested in combination with other dengue inhibitors.

Keywords: Dengue virus, luteolin, Traditional Chinese Medicine (TCM), dengue antiviral, virus maturation, furin inhibitor

1. Introduction

Dengue fever, a mosquito-borne viral disease, is caused by dengue virus (DENV), transmitted by female mosquitoes, mostly *A. aegypti*., and mainly found in tropical and sub-tropical regions, urban and semi-urban areas. Dengue has become a global burden with approximately 500,000 people with severe dengue symptoms needing hospital care annually and with a 2.5% mortality rate (WHO, 2015; Messina et al., 2014; Bhatt et al., 2013).

DENV is a member of the flavivirus genus belonging to the Flaviviridae family and is comprised of a single-stranded, plus-sense RNA genome approximately 11,000 nucleotides in length. The genomic RNA encodes 10 proteins: three structural proteins capsid (C), membrane (M), and envelope (E) and seven nonstructural proteins NS1, NS2A, NS2B, NS3, NS4A, NS4B, and NS5 (Kuhn et al., 2002).

Depending on the degree of cleavage of precursor membrane (prM) protein, DENV exists either as immature or mature infectious virions (Richter et al., 2014). Immature dengue viral particles display prM proteins on the virion surface and are non-infectious, while in mature virus particles the pro protein convertase furin cleaves the ‘pr’ moiety to secrete infectious virus from the cell (Zybert et al., 2008). Virus enters the cell by directly attaching to host cell receptors or through Fc receptors as immune complex with dengue-specific antibody and enters by receptor-mediated endocytosis. Fusion between viral and host endosomal membranes caused by low pH gives rise to the release of nucleocapsid into the cytoplasm (Seema & Jain., 2005). Released viral RNA is translated at the endoplasmic reticulum (ER) to produce a single polyprotein that is cleaved by viral and host proteases into three structural proteins and seven nonstructural proteins. Viral genomic RNA replication is carried out in the cytoplasm by viral enzymes and host proteins within discrete membrane invaginations (Mackenzie., 2005). The newly synthesized RNA is capped, methylated and subsequently packaged by capsid protein to form a nucleocapsid which buds into the ER, where immature progeny virion enveloped within prM-E

heterodimers is assembled (Ying et al., 2003). The immature virions traffic to the Golgi where the prM protein is cleaved by the host proprotein convertase furin within the *trans*-Golgi network to produce infectious mature virus particles that are released by exocytosis from the cell and ready to infect other cells (Screaton et al., 2015).

A mountain of work has been devoted to dengue drug discovery (Lim et al., 2013). Virus-specific inhibitors have been identified to target the E, Capsid, NS4B, protease, helicase, methyltransferase, and NS5 polymerase. Beyond that, inhibitors that target host factors, for instance, viral translation, host pyrimidine biosynthesis, host cholesterol synthesis, and cellular glucosidase, have been shown to be efficacious (Noble et al., 2010). Despite these advances there is no licensed drug for dengue fever at present.

Traditional Chinese medicines (TCM) continue to be widely used in eastern societies as a treatment for symptoms such as fever, pain, bloating, rashes, and its benefits are also being recognized by the growing numbers of TCM users in westernized societies seeking natural remedies. TCM formulations against viral infectious disease are also commonly available in China (He & Hou., 2013) and concoctions consisting of *Artemisia annua L, Lonicera japonica Thunb and Gardenia jasminoides Ellis* are believed to have good curative effect, especially on shortening the period of fever, relieving muscle pain symptoms, and contributing to the return of platelet and leukocyte numbers to the normal range (Yang et al., 2016). These claims have not been investigated in rigorous case-controlled clinical trials because of the lack of information on the underlying mechanism of action and complexity of the TCM formulations which may work on multiple targets (Yu et al., 2006). Nevertheless the discovery and clinical use of Qinghaosu (artemisinin) as an anti-infective drug for malaria (White et al., 2015; Tu, 2016) serves as a strong reminder on the need for detailed systematic studies of selected TCMs.

In an attempt to identify new antiviral substances active against dengue virus, we tested hundreds of crude extracts from TCM plants classified as antipyretic herbs, detoxifying herbs, blood cooling herbs or

involuntary perspiration inducing herbs (Li et al., 2015) and isolated 13 candidate compounds that were tested for antiviral activity in DENV infected cells or AG129 mice. We found that the widely occurring flavonoid, luteolin, that was isolated as one of the main components from the herb *Viola yedoensis Makino* inhibited DENV replication in cell culture and mice. Further studies showed that luteolin obstructs the later stages of DENV viral lifecycle in cells and restricts virus maturation process by inhibiting the host proprotein convertase furin in an uncompetitive mode as determined by *in vitro* biochemical assay. The *Viola yedoensis Makino* herb is widely used by TCM practitioners for clearing heat, relieving toxicity, and cooling blood (Oshima et al., 2013; Zhou et al., 2009; Pan et al., 2015; Ngan et al., 1988) and our finding that its main constituent luteolin (0.15mg/g) can inhibit a host enzyme opens the possibility TCMs may be a source for potential drugs against dengue fever.

2. Material and methods

2.1 Cells, virus and antibodies

Huh-7 (hepatocellular carcinoma cells, ATCC), Vero (African green monkey kidney cells, ATCC) and HEK-293T (Human Embryonic Kidney 293 cells, ATCC) cells were cultured in DMEM medium containing 10 % FBS, 1 % penicillin/streptomycin (P/S) at 37^{o}C in 5 % CO_2. BHK-21 (baby hamster kidney fibrolast cells, ATCC) cells were cultured in RPMI 1640 medium containing 10 % FBS, 1 % P/S, at 37 ^{o}C in 5 % CO_2. A549 (adenocarcinomic human alveolar basal epithelial cells, ATCC) cells were cultured in F12/K meduim containing 10 % FBS, 1 % P/S, at 37^{o}C in 5 % CO_2. C6/36, an *Aedesalbopictus* cell line (ATCC), was maintained in RPMI 1640 medium containing 25 mM HEPES, 10 % FBS and 1 % P/S, at 28 ^{o}C in the absence of CO_2. Hybridoma cell lines (ATCC) for 4G2 and 3H5 were grown in PFHM-II (Gibco) medium with 1% P/S at 37 ^{o}C in 5 % CO_2.

DENV-1 (EDEN-1, GenBank accession **EU081230**), DENV-2 (EDEN2, GenBank accession **EU081177**), DENV-3 (EDEN-3, GenBank accession **EU081190**) and DENV-4 (EDEN-4, GenBank accession **GQ398256**) were obtained from the Early Dengue infection and outcome (EDEN) study in Singapore

(Low et al., 2006). All virus strains were grown in C6/36 cells and the supernatants were stored at -80°C. Virus titer was determined by plaque assay on BHK-21 cells.

DENV-specific mouse monoclonal antibodies, 4G2 and 3H5 against E protein, were prepared from hybridoma cell lines as described previously (Watanabe et al., 2012).

2H2 against prM MAbs was a generous gift from Prof. Shee Mei Lok.

2.2 Extracts preperation

Two-gram of herb (KANGMEI Pharmaceutical Co. Ltd) was smashed and extracted with 20 ml distilled water by heating reflux extraction for 30 min or extracted with 20ml 70% ethanol by ultrasonic extraction for 30 min. The extracts were condensed under vacuum to obtain the residue and diluted with 20 ml of distilled water for antiviral activity assay.

2.3 Therapeutic compounds

Compounds in plant extracts (Purity > 95%) were purified and isolated by macro-reticular resin column (Cangzhou Bon Adsorber Technology Co. Ltd), RP-C18 column (Merck), sephadex LH-20 (Sigma) and reversed-phase preparative HPLC column (Phenomenex, 10 × 250 mm, 5μm) as described previously (Peng et al., 2016).

NITD008 used as a positive control for DENV infection was a generous gift from Novartis Institute for Tropical Disease, Singapore.

2.4 Cell viability assay

For measurement of compound cytotoxicity, Huh-7, A549, HEK-293T, BHK-21 and Vero cells, were seeded at 2×10^4 cells per well with 10 % FBS medium in 96-well white flat-bottom plate. Cells were incubated with various concentrations of compound for an additional 48 h. Cell viability was measured using CellTiterGlo® Luminescent cell viability Assay (Promega) kit according to the manufacturer's

instructions. Luminescence was measured on microplate reader (Tecan Infinite 200 PRO) with a 100 m/s integration time. For crude extracts, cell viability was measured using Cell Counting Kit-8 (Dojindo) according to the manufacturer manufacturer's instructions. Cell viability curve presented as percentage of luminescence derived from treated samples to that of the untreated control.

2.5 Virus infection

Huh-7 cells were seeded in a 24-well plate at 1×10^5 cells per well. Eight concentrations (50, 25, 12.5, 6.25, 3.125, 1, 0.1, 0.01 μM) were used to generate inhibition curve. Cells were infected with DENV strains at a multiplicity of infection (MOI) of 0.3 in the presence of compounds for 1 h. Virus/drug inoculums were removed and fresh medium containing the indicated concentrations of compounds was added. Cells were incubated for additional 48 h at 37°C and the supernatants were collected. Virus titers in the supernatants were determined by plaque assay using BHK-21 cells. EC_{50} was determined using GraphPad Prism software.

For antibody-dependent enhanced (ADE) infection, peripheral blood mononuclear cells (PBMCs) were isolated from human blood using Ficoll-Paque (GE Healthcare) extraction method according to manufacturer's instructions. DENV-1 (MOI of 10) and humanized 4G2 (0.05 μg) were mixed and incubated on ice for 1 h to allow the formation of immune complexes. PBMCs (1×10^6) were infected with the immune complexes for 2.5 h at 37°C with shaking. Cells were then washed once with PBS before resuspending in RPMI medium containing indicated concentrations of the compounds for a further incubation of 48h. After 48h, supernatants were harvested, subjected to virus titer determination by plaque assay and IL6 ELISA assay using Ready-Set-Go! ELISA kit (eBioscience) according to manufacturer's instructions.

2.6 Time of drug addition assay

To determine the mode of action of Luteolin, 1×10^5 Huh-7 cells were seeded into a 24-well plate and infected with DENV2 at MOI 1 for 1 h as described above. Infected cells were treated with 10μM of Luteolin either at 2h prior to infection or at 0, 2, 6, 12, 24 or 48 h p.i. Supernatants were collected by 48h p.i. for plaque quantification.

2×10^5 Huh-7 cells were seeded into a 12-well plate and incubated overnight at 37°C in 5% CO_2. Cells were infected with DENV2, then virus inoculums were removed and replaced with fresh medium. At 12h post infection (p.i), 10μM of Luteolin and control NITD008was added to the infected cells. Samples were harvested at 12, 24, 36 and 60 h p.i. Supernatants collected were used for quantification of virus titer measured by plaque assay and real time PCR. Cells were washed once with PBS and lysed with 500μl of Trizol (Invitrogen) for viral RNA quantification.

2.7 RNA extraction and RT-PCR

For intracellular viral RNA quantification, total RNA was isolated from cell lysate using the Trizol extraction method. 500 ng of total RNA was used for cDNA synthesis using ImProm II reverse transcription system (Promega) with random primers according to the manufacturer's instructions. 40 ng of cDNA was used for real-time PCR in Bio-Rad iQ-5 real time thermal cycler using SYBR green supermix (Bio-Rad). Primers binding to DENV2 E gene (Forward primer 5'-CAGGCTATGGCACTGTCACGAT-3', Reverse primer5'-CCATTTGCAGCAACACCATCTC-3') or the distal 3′UTR region (Forward primer 5'-CAGCATATTGACGCTGGGAAAGACC-3', Reverse primer5'-AGAACCTGTTGATTCAACAGCACCATTC) were used for amplification of the viral genome. Plasmid fragments containing DENV2- 3295 E gene or 3'UTR fragments were used to generate a standard curve for quantification of viral copy number. Results were reported as absolute viral genome copy per μg RNA normalized to actin expression. Viral RNA in the supernatant or mouse serum samples were extracted using QIAamp Viral RNA Mini Kit (Qiagen) according to the manufacturer's instructions. Real-time PCR was carried out in Bio-Rad iQ-5 real time thermal cycler using iTaq Universal SYBR

green one step kit (Bio-Rad) for supernatant and the DENV2 E primers as described above. For serum samples, qScript one-step qRT-PCR kit (Quanta) is used for RT-PCR with primers and TaqMan probes described previously (Watanabe et al., 2016). Absolute viral RNA genome copy was calculated based on the DENV standard curve and reported as absolute number of viral RNA genome copy per ml of supernatant (Tay., 2015). The limit of detection of real-time PCR is indicated as the grey dotted line in the graph.

2.8 Immunoprecipitation

Ten-microgram of mouse monoclonal antibody 3H5 (DENV2-specific anti-E) were used to coupled to 40 µl of protein A/G agarose beads (Thermo scientific) at 4^{o}C for 2h with rotation. Coupled beads were washed thrice with PBS-T (PBS with 0.1% Tween 20) to remove excess uncoupled antibody. 500 µl of supernatants from the time of addition experiment were added to the beads and incubated overnight at 4◦C with rotation. Beads were washed with PBS-T and proteins were eluted from the beads using 4× non-reducing buffer [0.2 M Tris-HCl (PH 6.8), 40 % glycerol, 8 % (wt/vol) SDS , 0.05 M EDTA, 0.08 % bromophenol blue]. The elutates were subjected to electrophoresis by 15 % SDS-PAGE gel without heat treatment. Proteins were transferred to PVDF membranes (Millipore) and nonspecific binding on the membrane was blocked with 3 % skim milk in PBST for 30 mins. The membrane was incubated with a mouse antibody (Mab) (2H2) specific for prM and 4G2 (anti-E) as an internal control at room temperature for 2 h with shaking. HRP-conjugated anti-mouse antibody was used for detection for 1 h at room temperature with shaking. Immunoreactive proteins were visualized using WesternBright Sirius HRP substrate (Advansta) and imaged on an ImageQuant instrument (Bio-Rad). The molecular weight sizes of protein bands were estimated by comparison with Precision Plus Protein Dual Color Standards (Bio-Rad). The integrated density of band was quantified by using ImageJ software.

2.9 Protease inhibition assay

Furin protease inhibition assay was performed in 384-well polystyrol microtiter plates in a 100 µl reaction mixture, containing 100 mM Hepes (pH 7.0), 0.5 % Triton X-100, and 0.5 mM $CaCl_2$. One unit of furin (New England Biolabs) and different concentrations of luteolin between 5 µM and 200 µM were pre-incubated at room temperature for 30 mins. Subsequently, substrate Pyr-Arg-Thr-Lys-Arg-AMC (Pyr = pyroglutamic acid, AMC = 7-amino-4-methyl coumarin; Bachem) at a final concentration of 100 µM was added. Fluorescence intensity was performed on the microplate reader (Tecan Infinite 200 PRO) at an excitation wavelength of 380 nm and emission wavelength of 460 nm at 37°C at 5-minute intervals of 1 h. Reaction rates were measured as RFU/s. The percent inhibition is calculated as following equation: Inhibition (%) = [(RFU/s) positive control- (RFU/s) inhibitor]/ (RFU/s) positive control ×100%. Data was analyzed using GraphPad Prism 5.

2.10 Ki determination

One unit of furin was pre-incubated with different concentration of luteolin ranging from 5 to 50 µM at room temperature for 30 mins before the addition of various concentrations of Pyr-RTKR-AMC substrate (50 µM, 100 µM, 250 µM, and 500 µM). Fluorescence intensity was measured by microplate reader (Tecan Infinite 200 PRO) at 37°C at 5-minute intervals for 1 h. Inhibition constant (Ki) was estimated from the intercept on the inhibitor concentration axis by using Dixon plots reporting the ratio of substrate concentration to velocity (s/v).

2.11 In vivo antiviral studies

Sv/129 mice deficient in type I and II interferon receptors (AG129), purchased from B&K Universal (UK), were housed in the BSL-2 animal facility at Duke-NUS, Singapore. All animal experiments were performed in conformity to Singapore National guidelines (protocol 2012/SHS/713) and approved by Institutional Animal Care and Use Committee at Singapore Health Services. Seven to eleven week-old male mice were administered with 50 µg of 4G2 antibody by intraperitoneal injection one day prior to infection with 1×10^8 pfu of DENV2 strain. Mice were treated with luteolin at 100mg/kg orally at

4/4/4/12h (9 AM, 1 PM, 5 PM and 9 PM on each day) cycle for a four times daily dosing from day 0 to day 4. Blood was collected by submandibular bleeding on day 1 to day 4 and serum samples were prepared for quantification of viral load by qRT-PCR as described in 2.6. Survival of mice was monitored until day 10 and survival curves were plotted in GraphPad Prism-5.

3. Results

3.1 identification of luteolin as an anti-DENV agent

The classification of herbs in the Chinese pharmacopeia summarized in Figure 1A provided the source for 70 herbs that were extracted with aqueous buffer (boiling) or 70% ethanol (sonication) that was used to discover molecules with anti-dengue viral activity (Fig.1B). The extracts were tested for anti-DENV properties in BHK-21 infection assay in conjunction with cell-viability assay (data not shown). From this study, five candidate extracts with more than 50% inhibition of cell-viability were selected (data not shown). Two of them are ethanol extracts from *Viola yedoensis Makino* and *Isatis indigotica Fortune* while three of them are aqueous extracts from *Picrorhiza scrophulariiflora Pennell*., *Paeonia suffruticosa Andr*. and *Lobelia chinensis Lour*.(Fig. 1C). Further purification by RP-HPLC and characterization of chemical structure by NMR identified total 13 compounds which were tested in DENV-2 infected Huh-7 cells at a single concentration of 10 μM. Viral titers in the treated or untreated culture medium were determined by plaque assay at 48 hours after infection (Fig.2A, Table 1). Of the compounds tested luteolin (compound 4, Fig. 2B) from *Viola yedoensis Makino* extract was found to drastically inhibit dengue virus infection with 20-fold reduction compared with virus only control and appeared to be comparable to the level of reduction obtained for NITD 008, a nucleoside inhibitor as control (Yin et al 2009). We also tested the anti-viral activity of luteolin in other cell lines. In contrast to Huh-7 cells, luteolin at the concentration of 10 μM did not show similar level reduction in viral titer for A549, BHK-21 or HEK-293T cells. Although luteolin demonstrates differential level of virus reduction across the cell

lines tested, we suspected that luteolin efficacy may be cell-type dependent and proceeded to obtain EC_{50} (concentration of compound inhibiting 50% of virus titer) in dose-response experiments (see below).

3.2 Luteolin is a potent inhibitor of DENV-1-4 and restricts ADE-Mediated infection in vitro

Next in order to test the antiviral efficacy of luteolin in inhibiting all four serotypes of DENV, Huh-7 cells were infected with DENV 1-4 in the presence of various concentrations of luteolin (50, 25, 12.5, 6.25, 3.125, 1, 0.1, 0.01 μM) and incubated for 48h, following which viral titers in the supernatants were measured by plaque assay. Luteolin inhibited DENV-2 in a dose-dependent manner in a viral titer reduction assay with an EC_{50} of 5.19 μM and selectivity index (SI) of 8.84 (Fig. 3B, Supplementary Fig. 2A). Significantly, luteolin was active against all four DENV serotypes with EC_{50} values of 7.2, 5.69, and 8.38μM and SI of 6.37, 8.07, and 5.48 for DENV-1, -3, and -4, respectively (Fig. 3A, 3C, 3D, Table 2 and Supplementary Fig. 2A). Luteolin also inhibited DENV-2 in various cells types, including A549, HEK-293T, BHK-21, and Vero cells albeit with EC_{50}s of 39.16, 12.26, 14.04, and 9.36, respectively (Table 2).

Since dengue is a lymphotropic disease, we set out to determine if luteolin will be active in inhibiting PBMCs infected with clinical strain of DENV-1 (Low et al., 2006) in the presence of humanized 4G2 (h4G2) antibody (Paradkar et al., 2011) thereby recapitulating the antibody-dependent enhancement (ADE) of DENV infection observed in severe cases (Halstead, 2007). Sub-neutralizing antibodies such as 4G2 facilitate DENV entry through monocytes via the Fc receptor (Littaua, 1990). Immune complex consisting of DENV-1 and h4G2 (Fraser et al., 2014) were performed *in vitro* and used to infect PBMCs. Infected PBMCs were subsequently incubated for 48 hours in the presence of luteolin (50, 25, 12.5, 6.25, 1, 0.1 μM) and found to inhibit viral replication with an EC_{50} of 15.61 μM and SI was 3.23 (Fig.3E, Table 2, Supplementary Fig. 2B).

3.3 Luteolin effectively reduces infectious DENV production by inhibiting viral maturation process

DENV life cycle has multiple potentially vulnerable points where suitable DENV therapeutics can be developed. To address this question, we performed time-of-drug-addition assay where 10 μM luteolin was added to DENV-2 infected Huh-7 cells either prior to time of infection or at five time points after infection followed by with viral titer quantification by plaque assay at 48 h post infection. The data indicated that luteolin was maximally effective when added at the time of infection. The level of infectious DENV released into the media from infected cells was still reduced even when luteolin treatment commence at 24 h post-infection, suggesting that luteolin affects the later stages of the virus lifecycle (Fig. 4).

To further investigate this phenomenon, infected Huh-7 cells were treated at 12 h pi with 10 μM luteolin or 10 μM NITD008 (Fig. 5A) and sampled at 24, 36, 60 h from 12 to 60 hours after infection. The intracellular and extracellular levels of DENV genome RNA were monitored at the various time points by real-time RT-PCR using E gene primers (Tay et al., 2015). The intracellular viral RNA levels for luteolin treatment or untreated DENV infection control cells increased gradually until 60 hours post infection, unlike the NITD008 treated cells which showed strong inhibition of RNA replication (Fig. 5B) as noted previously (Fraser et al., 2014). On the other hand the level DENV RNA detected in the extracellular supernatant samples from luteolin-treated cells were reduced 2 to 3-fold compared to DENV infection control (Fig.5C). Interestingly, furthermore detection of viral titer in the supernatant measured by plaque assay showed a dramatic reduction (15.5-fold at 60 h pi) in the infectious virus titer for the luteolin treated cells compared to the untreated cells (Fig. 5D), suggesting that luteolin reduces infectious virus particles formation but not viral RNA synthesis.

DENV maturation is associated with the status of M protein of virus particle where prM protein is cleaved by host proprotein convertase furin protease in *trans*-Golgi network (Zybert et al., 2008). Therefore, we analyzed the protein composition of virus particles by SDS-PAGE. Supernatants collected at 60 h were subjected to protein immunoprecipitation using 3H5 antibody that is specific for E protein to isolate prM protein. Consequently, a prominent prM band around molecular weight 20 kDa was detected in the

supernatants of luteolin treatment, showing that virus particles secreted from luteolin treated cells contained larger amount of prM protein. Next, we quantified the prM and E contents using ImageJ software by relating the integrated density of prM bands to that of E (Fig. 5E). The ratio of prM/E in virions with luteolin treatment was 13.3-fold higher than virus control (at 60h pi), revealing that most of the virus particles secreted from treated cells were immature prM-containing viruses.

The expression of E and NS5 protein were analyzed by indirect immunofluorescence assay on DENV 2 infected Huh7 cell that were treated with luteolin 12 hours post infection. There was no difference between the luteolin treatment and virus control, implying that luteolin was unable to inhibit protein synthesis as NITD008 inhibits in huh-7 cells (data not shown). Taken together, the data suggests that luteolin cannot inhibit the viral replication stage but exerts its inhibitory action on the virus maturation process by preventing the conversion of prM to M protein.

3.4Luteolin is an uncompetitive inhibitor against furin protease activity in vitro

In order to biochemically characterize the mechanism of action of luteolin, a furin cleavage inhibition assay was conducted as described (Zhu et al., 2013). The enzymatic reaction involving the cleavage of the substrate pyr-RTKR-AMC with the human proprotein convertase furin isolated from Sf9 cells infected with recombinant baculovirus carrying truncated human furin (NEB), was followed using a flurometirc assay with an excitation wavelength of 380 nm and emission wavelength of 460 nm (Fig. 6A). The rate of catalysis increased linearly as substrate concentration increased and then began to level off and approach a maximum at higher substrate concentrations with the amount of the furin being kept constant (one unit). This confirms that the furin is enzymatically active based on the increase in reaction rate that accompanies the cleavage to release the fluorescent AMC moiety. To examine the inhibition by luteolin, a concentration range of 5 to 200 μM was tested on the catalytic activity of human furin enzyme (1 unit) at a substrate concentration of 100 μM. A dose dependent inhibition effect on furin cleavage was observed. Maximal inhibition of the enzyme activity (>95%) was achieved at a concentration of 200 μM (Fig. 6B).

To determine the kinetic parameters, various concentrations of luteolin and the substrate pyr-RTKR-AMC were tested. The characteristic of the resulting Lineweaver-Burk double reciprocal plot and Dixon plots indicated that luteolin was an uncompetitive inhibitor, where inhibition occurs through binding to the enzyme-substrate complex rather than enzyme itself, with inhibitor constant (Ki) value of 58.6 μM (Fig. 6C, D). These results suggest that luteolin acts on furin-substrate complex to restrict the cleavage product formation, proving that virus maturation, which requires furin processing, was prevented under the treatment of luteolin.

3.5 Luteolin can reduce viremia in mouse model of DENV infection

The lethal ADE infection mouse model using DENV2 clinical isolate (Watanabe et al., 2016) was used to evaluate the *in vivo* efficacy of luteolin. Mice were treated orally with 100mg/kg of luteolin for 5 days, beginning with the day of infection. Four times daily luteolin treatment was sufficient to protect 33% of mice (Fig. 7A), while viremia level displayed a 2.2-fold reduction on day 4 (Fig. 7B, 7C) compared to virus control mice. On the whole, our data suggest that luteolin can inhibit DENV *in vivo*. The lack of 100% protection may be indicative of the competing processes in the infection model but the 2.2 fold reduction in viremia at day 4 pi is pointing in the right direction although it is not statistically significant.

4. Discussion

The search for new antivirals from extracts of TCM herbs that have a long history of application in human diseases is a potentially worthy approach as it can lead to new discoveries. We picked 70 herbs that are commonly used by TCM practitioners for a wide range of ailments. Aqueous extracts by reflux from *Picrorhiza scrophulariiflora Pennell*. (containing iridoid glycoside, phenolic glycoside, phenylethanoid glycoside, etc) (He et al., 2012), *Paeonia suffruticosa Andr*. (rich in monoterpene, phenolic glycoside, triterpenoid, etc) (Cao, 2013) and *Lobelia chinensis Lour*. (containing alkaloid, flavone, coumarin , etc) (Wang et al., 2013) and ethanol extracts by sonication from *Viola yedoensis Makino.* (flavone, coumarin,

organic acid, etc) (Li et al., 2013) and *Isatis indigotica Fortune.* (consisting of isdirubin, indigo, isoindigo, etc) (Li, 1987) were shown to possess antiviral activity, which led to purification of 13 compounds.

Luteolin, purified from *ViolayedoensisMakino*., a naturally occurring flavone with broad activities including suppressing tumor cell proliferation, inducing tumor cells apoptosis, anti-inflammatory as well as antioxidant properties (Nabavi et al., 2015), was characterized further for inhibitory activity against DENV. We found that purified luteolin has different antiviral efficacy against different cell types, where the efficacy of luteolin is comparable in HEK-293T, A549, and BHK-21, but different in Huh-7 as well as Vero cells. Nevertheless the compound was active against the cell lines in the EC_{50} range of 5.4-39.16 μM. We further examined the antiviral activity of luteolin against ADE-mediated infection using human PBMCs with enhancing concentration of 4G2 antibody, and showed that it is able to prevent infection *in vitro* with an EC_{50} 15.61 μM. However the inhibitory effect of the directly acting antiviral (adenosine nucleoside inhibitor) NITD008 is fairly consistent in each cell lines and its efficacy in the PBMC assay is around 0.46 μM. Cell-type variability in EC_{50} was also observed for celgosivir (butyl-castanospermine) (Watanabe et al., 2016), which is a prodrug of the natural product castanospermine that inhibits cellular alpha-glucosidase and misfolds prM, E, as well as NS1 (Whitby et al., 2005; Rathore et al., 2011; Schul et al., 2007), but the mechanistic basis for the difference and whether this has clinical significance are not clear.

Mature virus enters the cell by receptor mediated endocytosis and following membrane fusion, the viral RNA genome is translated, post-translationally processed to carry out replication and packaged. One important step in the production of infectious virion that takes place prior to egress from the infected cell occurs in the *trans*-Golgi network, where the prM protein is cleaved by host proprotein convertase furin protease, leading to an anchored membrane M stump and a "pr" peptide that remains linked with the virus particle until it is secreted (Li et al., 2008; Kostyuchenko et al., 2013). As soon as it egresses from the host cell, the pr peptide disassociates to turn the inert virus into an infectious particle. We found that luteolin disrupts the later stages of dengue viral lifecycle in cells by inhibiting the host proprotein

convertase furin in an uncompetitive mode, resulting in inefficient cleavage of prM protein. As a consequence, virus maturation process is interfered and less mature virus particles are produced, which could effectively reduce or arrest subsequent viral infection. The *in vitro* inhibition in various cell-lines as well as PBMCs shown in this study appears to be due to the accumulation of immature particles (Fig. 5E). The data in the mouse model of infection was modest but the reduction in viremia that was observed and the lowering of cytokine interleukin 6 (IL-6) in ADE-mediated DENV-infected PBMCs (Supplementary Fig. 3) collectively suggest that luteolin treatment may resolve viremia and also reduce the secretion of inflammatory cytokines associated with DENV infection.

The present study also validates the host enzyme furin as a target for antiviral development. Furin is a member of the family of highly specific, calcium-dependent proprotein/prohormone convertases (PCs) (Seidah et al., 1998) that recognize the cleavage sequence -Arg-X- X-Arg ↓- (where Lys is lysine, X is any amino acid and ↓ identifies the cleavage site) (Krysan et al., 1999). Furin aggregates in *trans*-Golgi network and follows a highly regulated transport thread through several TGN/endosomal compartments and cell surface (Molloy et al., 1999), which accounts for how it deals with multiple proprotein substrates in the cell. Importantly, furin plays a key role in activating several viruses eg. respiratory syncytial virus, influenza virus, measles virus , HIV-1 and flavivriruses (Molloy et al., 1999) by proteolytic cleavage of surface proprotein (prM in the case of flaviviruses). Interestingly the cleavage specificity of furin bears some resemblance to the recognition sequence of DENV NS2B/NS3 (Li et al., 2005) in that the P1 residue is an Arg. Biochemical testing of purified DENV2 NS2B/NS3 protease showed that luteolin is a much weaker inhibitor of the viral protease with a Ki of 140.36 μM (Supplementary Fig. 4A, B, C & D). Since the IFA staining showed no difference in the level of viral proteins (E, NS3 and NS5; data not shown) in the time-of-addition-assay, it can be surmised that the blocking of furin activity by luteolin is probably the main mechanism of inhibition.

Luteolin which forms 0.15mg/g of TCM herb *yedoensis Makino* is shown in this work to be active *in vivo* with a modest 33% survival rate and 2.2-fold reduction in viremia at day 4 pi thereby supporting the *in*

vitro efficacy data. The lack of 100% protection may be due to low potency and other issues such as the low bioavailability (Nordeen et al., 2013). Further studies to explore more potent inhibitors could involve structure-based approaches in the light of recent structural studies carried out with this enzyme (Dahms et al., 2016).

Our results show, for the first time, that the natural product luteolin originating from heat clearing herbs which is traditionally used by TCM physicians for fever treatment has the potential to be developed as a new drug against dengue virus infection. There are only a few of cases where TCM herbs have been successfully developed into important drugs, and the example of the antimalarial substance artemesinin from the herb *Artemisia annua* extract stands out as a great success story (Miller et al., 2011). Our studies show that the approach to examine TCM herbs has potential to find more valuable medicines that can be used to treat diseases including viral or viral infections.

Acknowledgements

We thank Drs Jenny Low and Crystall Swarbrick for comments on the manuscript. This work is supported by the Guangdong Natural Science Foundation (No. S2012030006598), the Science & Technology Planning Project of Guangdong Province of China (No. 2013A020229007), Financial Grant from the China Postdoctoral Science Foundation (2016M592477). An International PhD Student Travel Award was made to Minhua Peng (A1-AFD018161Z0102). This work is in part supported by NMRC grant no. NMRC/CBRG/0103/2016 awarded DL and SGV by Singapore Ministry of Health.

Reference

Bhatt, S., Gething, P.W., Brady, O.J., Messina, J.P., Farlow, A.W., Moyes, C.L., Drake, J.M., Brownstein, J.S., Hoen, A.G., Sankoh, O., Myers, M.F., George, D.B., Jaenisch, T., Wint, G.R., Simmons, C.P., Scott, T.W., Farrar, J.J., Hay, S.I., 2013. The global distribution and burden of dengue. Nature. 496, 504–507.

Birdee, G.S., Wayne, P.M., Davis, R.B., Phillips, R.S., Yeh, G.Y., 2009.T'ai chi and qigong for health: patterns of use in the United States. J Altern Complementary Med. 15, 969–973

Cao, C.Q., 2013. Advances on chemical constituents of Chinese moutan cortex. Guangzhou chemical industry (in Chinese). 12, 44–51.

Chan, E., Tan, M., Xin, J.,Sudarsanam, S., Johnson, D.E., 2010. Interactions between traditional Chinese medicines and Western therapeutics. CurrOpin Drug DiscovDevel. 13, 50–65.

Chang, W.C., Hsu, F.L., 1992. Inhibition of platelet activation and endothelial cell injury by polyphenolic compounds isolated from Lonicera japonica Thunb. Prostaglandins Leukot Essent Fatty Acids. 45, 307–312.

Dahms, S.O., Arciniega, M., Steinmetzer, T., Huber, R., Than, M.E., 2016. Structure of the unliganded form of the proprotein convertase furin suggests activation by a substrate-induced mechanism. Proc Natl Acad Sci U S A. 113, 11196–11201.

Fraser, J.E., Watanabe. S., Wang. C., Chan, W.K., Maher, B., Lopez-Denman, A., Hick, C., Wagstaff, K.M., Mackenzie, J.M., Sexton, P.M., Vasudevan, S.G., Jans, D.A., 2014. A nuclear transport inhibitor that modulates the unfolded protein response and provides in vivo protection against lethal dengue virus infection. J Infect Dis. 210, 1780–1791.

Halstead SB., 2007. Dengue. Lancet. 370, 1644–1652.

He, J., Hou, X.Y., 2013. The potential contributions of traditional Chinese medicine to emergency medicine. World J Emerg Med. 4, 92–97.

He, X.R., Li, Q., Zhang, C.L., Chang, Y., Yao, H., Zhao, T., 2012. Phytochemical and biological studies on *Picrorhiza scrophulariiflora Pennell*. Global traditional Chinese medicine (in Chinese). 9, 708–713.

Heh, C.H., Othman, R., Buckle, M.J., Sharifuddin, Y., Yusof, R., Rahman, N.A., 2013. Rational discovery of dengue type 2 non-competitive inhibitors. Chem Biol Drug Des. 82, 1−11.

Kostyuchenko, V.A., Zhang, Q., Tan, J.L., Ng, T.S., Lok, S.M., 2013. Immature and mature dengue serotype 1 virus structures provide insight into the maturation process. J Virol. 87, 7700–7707.

Krysan, D.J., Rockwell, N.C., Fuller, R.S., 1999. Quantitative characterization of furin specificity. Energetics of substrate discrimination using an internally consistent set of hexapeptidyl methylcoumarinamides. J.Biol. Chem. 274, 23229–23234.

Kuhn, R.J., Zhang, W., Rossmann, M.G., Pletnev, S.V., Corver, J., Lenches, E., Jones, C.T., Mukhopadhyay, S., Chipman, P.R., Strauss, E.G., Baker, T.S., Strauss, J.H, 2002. Structure of dengue virus: implications for flavivirus organization, maturation, and fusion. Cell. 108, 717−725.

Li, J., Lim, S.P., Beer, D., Patel, V., Wen, D., Tumanut, C., Tully, D.C., Williams, J.A., Jiricek, J., Priestle, J.P., Harris, J.L., Vasudevan, S.G., 2005. Functional profiling of recombinant NS3 proteases from all four serotypes of dengue virus using tetrapeptide and octapeptide substrate libraries. J Biol Chem. 280, 28766−28774.

Li, J.Q., Gu, X.Z., Liu, Y.T., Zhang, Z.D., 2015. Diagnosis and treatment of dengue fever in Guangzhou from 2014 to talk about the practice of Chinese medicine treatment of dengue Experience. Jiangsu Traditional Chinese Medicine (in Chinese). 7, 16−18.

Lim, S.P., Wang, Q.Y., Noble, C.G., Chen, Y.L., Dong, H., Zou, B., Yokokawa, F., Nilar, S., Smith, P., Beer, D., Lescar, J., Shi, P.Y., 2013. Ten years of dengue drug discovery: progress and prospects. Antiviral Res. 100, 500–519.

Lin, L.C., Pai, Y.F., Tsai, T.H., 2015. Isolation of Luteolin and Luteolin-7-O-glucoside from Dendranthema morifolium Ramat Tzvel and Their Pharmacokinetics in Rats. J Agric Food Chem. 63, 7700–7706.

Low, J.G., Ooi, E.E., Tolfvenstam, T., Leo, Y.S., Hibberd, M.L., Ng, L.C., Lai, Y.L., Yap, G.S., Li, C.S., Vasudevan, S.G., Ong, A., 2006. Early Dengue Infection and Outcome Study (EDEN) - Study Design and Preliminary Findings. Ann Acad Med Singapore. 35, 783–789.

Low, J.G., Sung, C., Wijaya, L., Wei. Y., Rathore, A.P., Watanabe, S., Tan, B.H., Toh, L., Chua, L.T., Hou, Y., Chow, A., Howe, S., Chan, W.K., Tan, K.H., Chung, J.S., Cherng, B.P., Lye, D.C., Tambayah, P.A., Ng, L.C., Connolly, J., Hibberd, M.L., Leo, Y.S., Cheung, Y.B., Ooi, E.E., Vasudevan, S.G., 2014. Efficacy and safety of celgosivir in patients with dengue fever (CELADEN): a phase 1b, randomised, double-blind, placebo-controlled, proof-of-concept trial. 14, 706–715.

Mackenzie, J., 2005. Wrapping things up about virus RNA replication. Traffic. 6, 967–977.

Messina, J.P., Brady, O.J., Scott, T.W., Zou, C., Pigott, D.M., Duda, K.A., Bhatt, S., Katzelnick, L., Howes, R.E., Battle, K.E., Simmons, C.P., Hay, S.I., 2014. Global spread of dengue virus types: mapping the 70 year history. Trends Microbiol. 22, 138–146.

Miller, L.H., Su, X.Z., 2011.Artemisinin: Discovery from the Chinese Herbal Garden. Cell. 146, 855–858.

Molloy, S.S., Anderson, E.D., Jean, F., Thomas, G., 1999. Bi-cycling the furin pathway: from TGN localization to pathogen activation and embryogenesis. Trends Cell Biol. 9, 28–35.

Nabavi, S.F., Braidy, N., Gortzi, O., Sobarzo-Sanchez, E., Daglia, M., Skalicka-Woźniak, K., Nabavi, S.M., 2015. Luteolin as an anti-inflammatory and neuroprotective agent: A brief review. Brain Res Bull. 119, 1−11.

Ngan, F., Chang, R.S., Tabba, H.D., Smith, K.M., 1988.Isolation,purification and partial characterization of an active anti-HIV compound from the Chinese medicinal herb Viola yedoensis. Antiviral Res. 10, 106−107.

Noble, C.G., Chen, Y.L., Dong, H., Gu, F., Lim, S.P., Schul, W., Wang, Q.Y., Shi, P.Y., 2010. Strategies for development of Dengue virus inhibitors. Antiviral Res. 85, 450–462.

Nordeen, S.K., Bona, B.J., Jones, D.N., Lambert, J.R., Jackson. T.A., 2013. Endocrine disrupting activities of the flavonoid nutraceuticals luteolin and quercetin. Horm. Cancer. 4, 293–300.

Oshima, N., Narukawa, Y., Takeda, T., Kiuchi, F., 2013.Collagenase inhibitors from Viola yedoensis. J Nat Med. 67, 240−245.

Pan, Y.Y., Song, Z.P., Zhu, G.F., Zhu, Y.Z., Lu, Y., Li, W.L., Gao, J., Cheng, Z.H., 2015. Antipyretic Effects of Liposoluble Fractions of Viola yedoensis.Chinese Herbal Medicines. 7, 80−87.

Paradkar, P.N., Ooi, E.E., Hanson, B.J., Gubler, D.J., Vasudevan, S.G., 2011. Unfolded protein response (UPR) gene expression during antibody-dependent enhanced infection of cultured monocytes correlates with dengue disease severity. Biosci Rep. 31, 221–230.

Peng, M.H., Dai, W.P., Liu, S.J., Yu, L.W., Wu, Y.N., Liu, R., Chen, X.L., Lai, X.P., Li, X., Zhao, Z.X., Li, G., 2016. Bioactive glycosides from the roots of Ilex asprella. Pharm Biol. 54, 2127–2134.

Li, L., Lok, S.M., Yu, I.M., Zhang, Y., Kuhn, R.J., Chen, J., Rossmann, M.G., 2008. The flavivirus precursor membrane-envelope protein complex: structure and maturation. Science. 319(5871):1830-4.

Li, Q.H., 1987. Chemical constituents of indigo naturalis. Journal of integrative plant biology (in Chinese).

Li, Y.S., He, X.R., Yang, Y., Zhang, C.L., Chang, Y., He, Rui., 2013.Study advancement about chemical composition and pharmacological action of *Viola yedoensis*. Global traditional Chinese medicine (in Chinese). 4, 313–318.

Littaua, R., Kurane, I., Ennis, F.A., 1990. Human IgG Fc receptor II mediates antibody-dependent enhancement of dengue virus infection. J. Immunol. 144, 3183–3186.

Rathore, A.P., Paradkar, P.N., Watanabe, S., Tan, K.H., Sung, C., Connolly, J.E., Low, J., Ooi, E.E., Vasudevan SG., 2011. Celgosivir treatment misfolds dengue virus NS1 protein, induces cellular pro-survival genes and protects against lethal challenge mouse model. Antiviral Res. 92, 453–460.

Richter, M.K., da Silva Voorham, J.M., Torres Pedraza, S., Hoornweg, T.E., van de Pol, D.P., Rodenhuis-Zybert, I.A., Wilschut, J., Smit, J.M., 2014. Immature dengue virus is infectious in human immature dendritic cells via interaction with the receptor molecule DC-SIGN. PLoS One. 9, e98785.

Schul, W., Liu, W., Xu, H.Y., Flamand, M., Vasudevan, S.G., 2007. A dengue fever viremia model in mice shows reduction in viral replication and suppression of the inflammatory response after treatment with antiviral drugs. J Infect Dis.195, 665–674.

Screaton, G., Mongkolsapaya, J., Yacoub, S., Roberts, C.,2015.New insights into the immunopathology and control of dengue virus infection.Nat Rev Immunol.15,745–759.

Seema., Jain, S.K., 2005.Molecular mechanism of pathogenesis of dengue virus: Entry and fusion with target cell. Indian J Clin Biochem. 20, 92–103.

Seida, N.G., Day, R., Marcinkiewicz, M., Chretien, M., 1998. Precursor convertases: an evolutionary ancient, cell-specific, combinatorial mechanism yielding diverse bioactive peptides and proteins. Ann. N. Y. Acad. Sci. 839, 9–24.

Tay, M.Y., Saw, W.G., Zhao, Y., Chan, K.W., Singh, D., Chong, Y., Forwood, J.K., Ooi, E.E., Grüber, G., Lescar, J., Luo, D., Vasudevan, S.G., 2015. The C-terminal 50 amino acid residues of dengue NS3 protein are important for NS3-NS5 interaction and viral replication. J Biol Chem. 290, 2379–2394.

Thomas, G., 2002. Furin at the cutting edge: from protein traffic to embryogenesis and disease. Nat Rev Mol Cell Biol. 3, 753–766.

Tu, Y., 2016. Artemisinin-A Gift from Traditional Chinese Medicine to the World (Nobel Lecture). Angew Chem Int Ed Engl. 55, 10210–10226.

WHO, 2015.Dengue and severe dengue.

Xie, C., Veitch, N.C., Houghton, P.J., Simmonds, M.S., 2003. Flavone C-glycosides from Viola yedoensis MAKINO. Chem Pharm Bull (Tokyo). 51, 1204–1207.

Yang, Z.Q., Xian. S.X., Liu, N., Zhang,W., Liu,Z.H., Yu, H., Xiao, W., 2016. Clinical Trial of Efficacy and Safety of Reduning Injection in Treating Common Type Dengue Fever.Traditional Chinese Drug Research and Clinical Pharmacology (in Chinese).1, 135–138.

Yin, Z., Chen, Y.L., Schul, W., Wang, Q.Y., Gu, F., Duraiswamy, J., Kondreddi, R.R., Niyomrattanakit, P., Lakshminarayana, S.B., Goh, A., Xu, H.Y., Liu, W., Liu, B., Lim, J.Y., Ng, C.Y., Qing, M., Lim, C.C., Yip, A., Wang, G., Chan, W.L., Tan, H.P., Lin, K., Zhang, B., Zou, G., Bernard, K.A., Garrett, C., Beltz, K., Dong, M., Weaver, M., He, H., Pichota, A., Dartois, V., Keller, T.H., Shi, P.Y.,.2009. An adenosine nucleoside inhibitor of dengue virus. Proc Natl Acad Sci U S A. 106, 20435–20439.

Yu, L., Luo, J., Tan, X., 2006. The basic research ideas of herbal prescription composing principles.Traditional Chinese Drug Research & Clinical Pharmacology (in Chinese). 16, 43–45.

Wang, P.P., Luo, J., Yang, M.H., Kong, L.Y., 2013. Chemical constituents of *Lobelia chinensis*. Chinese traditional and herbal drugs (in Chinese). 7, 794–797.

Watanabe, S., Chan, K.W., Dow, G., Ooi, E.E., Low, J.G., Vasudevan, S.G., 2016. Optimizing celgosivir therapy in mouse models of dengue virus infection of serotypes 1 and 2: The search for a window for potential therapeutic efficacy. Antiviral Res. 127, 10–19.

Watanabe, S., Tan, K.H., Rathore, A.P., Rozen-Gagnon, K., Shuai, W., Ruedl, C., Vasudevan, S.G., 2012.

The magnitude of dengue virus NS1 protein secretion is strain dependent and does not correlate with severe pathologies in the mouse infection model. J Virol. 86, 5508–5514.

White, N.J., Hien, T.T., Nosten, F.H., 2015. A Brief History of Qinghaosu. Trends Parasitol. 31, 607–610.

Whitby, K., Pierson, T.C., Geiss, B., Lane, K., Engle, M., Zhou, Y., Doms, R.W., Diamond, MS., 2005. Castanospermine, a potent inhibitor of dengue virus infection in vitro and in vivo. J Virol. 79, 8698–706.

Zhang, Y., Corver, J., Chipman, P.R., Zhang, W., Pletnev, S.V., Sedlak, D., Baker, T.S., Strauss, J.H., Kuhn, R.J., Rossmann, M.G., 2003. Structures of immature flavivirus particles. EMBO J. 22, 2604–2613.

Zhou, H.Y., Hong,J.L., Shu, P., Ni, Y.J., Qin, M.J., 2009. A new dicoumarin and anticoagulant activity from Viola yedoensisMakino.Fitoterapia. 80, 283–285.

Zhou, Y., Wang, Y., Wang, R., Guo, F., Yan, C., 2008. Two-dimensional liquid chromatography coupled with mass spectrometry for the analysis of Lobelia chinensis Lour. using an ESI/APCI multimode ion source. J Sep Sci. 31, 2388–2394.

Zhu, J., Van de Ven, W.J., Verbiest, T., Koeckelberghs, G., Chen, C., Cui, Y., Vermorken, A.J., 2013. Curr Med Chem. Polyphenols can inhibit furin in vitro as a result of the reactivity of their auto-oxidation products to proteins. 20, 840–50.

Zybert, I.A., van der Ende-Metselaar, H., Wilschut, J., Smit, J.M., 2008. Functional importance of dengue virus maturation: infectious properties of immature virions. J Gen Virol. 89, 3047–3051.

Figure legends

Figure 1. Identification of luteolin, a potent anti-dengue virus agent.

A, Classification of 70 kinds of herbs that were used for the extraction.

B, Flowchart showing the strategy for crude extracts screening and compounds isolation.

C, Photograph showing that five Chinese herbs exhibited anti-DENV activity were selected.

Figure 2. Anti-DENV activity of 13 purified compounds in Huh-7 cells.

A, Huh-7 cells were infected with DENV-2 at a MOI of 0.3 in the presence of 10 μM of the purified compounds and the viral titers in the supernatants at 48 h pi were determined by plaque assay, represented as plaque-forming units (PFU) per milliliter. 1 (Quercetin), 2 (Indirubin), 3 (Rutin), 4 (luteolin), 5 (Picroside II), 6 (Scopoletin), 7 (Vanillic acid), 8 (Cinnamic acid), 9 (Apigenin), 10 (Ursolic acid), 11 (Esculetin), 12 (Cichoric acid), 13 (Paeonol), 14 (NITD008), 15 (Virus control). Data are the mean ± standard deviation of two independent experiments.

B, Chemical structures of luteolin that showed good inhibitory efficacy against DENV-2.

Figure 3. Effect of luteolin against four serotypes (DENV-1-4) and ADE-Mediated infection in vitro. (luteolin: solid line, circle filled symbol; NITD008: dash line, triangle symbol)

A-D, Inhibitory effect of luteolin on DENV-1-4 in Huh-7 cells. Huh-7 cells were infected with DENV-1 (A), DENV-2 (B), DENV-3 (C) and DENV-4 (D) at a MOI of 0.3 in the presence of indicated concentrations of compounds and virus titers in the supernatants were determined by plaque assay. The bar indicates the standard deviation of two independent experiments.

E, Inhibitory effect of luteolin on ADE-Mediated infection of DENV-1 in PBMCs. DENV-1 with antibody 4G2 was infected in PBMCs at a MOI of 10 and the supernatants were collected at 48 h pi to

determine the virus titers by plaque assay. The bar indicates the standard deviation of two independent experiments.

Figure 4. I**nhibition of luteolin on the specific steps of DENV lifecycle.**

DENV-2 infected Huh-7 cells were treated with 10 μM luteolin or NITD008 either at 2h prior to infection or at 0, 2, 6, 12, 24 or 48h p.i., and virus titers in the supernatants were determined by plaque assay at 48 h pi. The data are mean ± standard deviation from two independent experiments.

Figure 5. Analysis for mode of action of luteolin on DENV replication cycle.

A, Schematic diagram showing the strategy for the experiments. (Luteolin: red solid line, square filled symbol; NITD008: blue solid line, triangle down symbol; Virus control: black solid line, diamond filled symbol)

B-D, 10μM of luteolin or NITD008 was added at 12 hours after infection with DENV-2 in Huh-7 cells. Cells were lysed at the indicated time intervals and absolute number of intracellular viral RNA genome copy was measured by realtime RT-PCR (B). Simultaneously, supernatants were collected and virus titers were measured by realtime RT-PCR to determine the absolute number of secreted viral RNA genome copy (C) or by plaque assay to determine the infectious virus levels (D). The bar indicates the standard deviation of two independent experiments.

E, Supernatants were collected at 60 hours after infection and subjected to protein immunoprecipitation to isolate prM protein. Western bolt was performed to visualize the amount of viral proteins in the supernatants analysis using antibodies directed toward E and prM protein.

Figure 6. Kinetic analysis of the luteolin inhibition of furin protease activity

A, Michaelis-Menten plot analysis of the luteolin inhibition of furin. One unit of furin was mixed with various concentrations of Pyr-RTKR-AMC substrate (25 μM, 50 μM, 100 μM, 250 μM, and 500 μM). Reaction rates were measured as RFU/s.

B, Inhibition profiles of luteolin on furin-mediated cleavage of the fluorogenic peptide Pyr-RTKR-AMC. One unit of furin and different concentrations of luteolin between 5 μM and 200 μM were pre-incubated at room temperature for 30 mins before the addition of 100 μM Pyr-RTKR-AMC substrate. The data are mean ± standard deviation from two independent experiments.

C, Lineweaver-Burk plot analysis of the luteolin inhibition of furin was yielded by double reciprocal plotting of 1/velocity versus 1/substrate.

D, Dixon plots for the inhibition of furin by luteolin. The substrate/velocity is plotted against the inhibitor concentration.

Figure 7. **Efficacy of luteolin against lethal infection of DENV-2 *in vivo*.** Six AG129 mice per group were pre-injected i.p. with 4G2 antibody followed by next day infection i.v. with 1×10^{8}pfu of DENV-2. The infected mice were orally administered luteolin four times per day at 100mg/kg for 5 days, beginning one hour before infection (on day 0).

A, mouse survival rate was monitored by day 10 pi.

B, Blood samples were collected on day 1-4 pi and serum from each mouse was subjected to real-time PCR to obtain the viral genome copy numbers.

C, Viremia level on day 4 pi. Viral copy number was measured individually and shown in the graphs as the mean ± standard deviation.

Table 1 Antiviral activity of 13 compounds against DENV-2

NO.	Chemical name	Structure	Reduction at 10 μM (fold)				Origin of plant
			Huh-7	BHK-21	A549	HEK-293T	
			MOI=0.3	MOI=0.3	MOI=0.3	MOI=1	
1	Quercetin	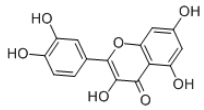	1.51 ± 0.04	1.23 ± 0.02	0.40 ± 0.10	2.20 ± 0.90	*Viola yedoensis Makino.*
2	Indirubin	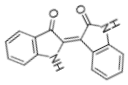	4.44 ± 0.35	1.76 ± 0.01	1.21 ± 0.27	2.02 ± 0.51	*Isatis indigotica Fortune.*
3	Rutin	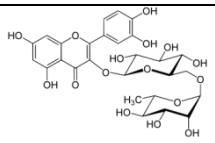	1.20 ± 0.25	0.87 ± 0.1	0.57 ± 0.08	1.32 ± 0.01	*Viola yedoensis Makino.*
4	luteolin	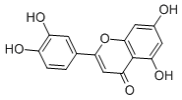	20.01 ± 0.71	1.18 ± 0.03	1.01 ± 0.21	2.44 ± 0.21	*Viola yedoensis Makino.*
5	Picroside II	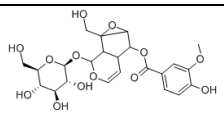	1.36 ± 0.20	1.09 ± 0.09	0.89 ± 0.19	1.92 ± 0.09	*Picrorhiza scrophulariiflora Pennell.*
6	Scopoletin	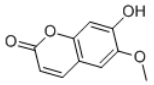	1.57 ± 0.09	1.04 ± 0.01	2.83 ± 0.54*	2.34 ± 0.19	*Viola yedoensis Makino.*
7	Vanillic acid	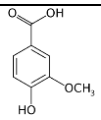	1.98 ± 0.10	1.34 ± 0.04	0.55 ± 0.02	1.65 ± 0.06	*Picrorhiza scrophulariiflora Pennell.*
8	Cinnamic acid	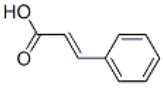	1.14 ± 0.00	1.56 ± 0.05	0.90 ± 0.34	1.21 ± 0.20	*Picrorhiza scrophulariiflora Pennell.*
9	Apigenin	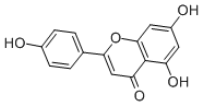	2.85 ± 0.49	1.19 ± 0.07	0.91 ± 0.49	1.89 ± 0.13	*Lobelia chinensis Lour.*

10	Ursolic acid	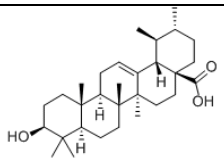	4.58 ± 0.18*	1.13 ± 0.01	8.00 ± 1.95*	14.20 ± 0.96*	*Viola yedoensis Makino.*
11	Esculetin	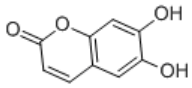	3.28 ± 0.74	1.47 ± 0.42	0.57 ± 0.08	1.73 ± 0.11	*Viola yedoensis Makino.*
12	Cichoric acid	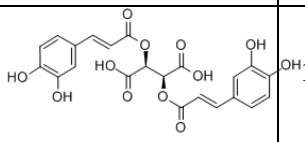	1.68 ± 0.13	1.70 ± 0.03	1.44 ± 0.18*	1.52 ± 0.40	*Viola yedoensis Makino.*
13	Paeonol	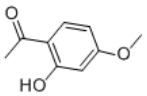	1.36 ± 0.30	1.16 ± 0.03	0.84 ± 0.13	1.46 ± 0.15	*Paeonia suffruticosa Andr.*
14	NITD008	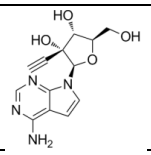	Very high	Very high	17.41 ± 1.89	Very high	

Cells were infected with DENV-2 and treated with 10 μM of indicated compounds. At 48 h post-infection, supernatants were collected and viral titer was measured by plaque assay. The data are mean ± standard deviation from two independent experiments.

*compound was toxic in the indicated cells.

Table 2 Cell toxicity and antiviral activity of luteolin against DENV

Cell type	MOI	Compound	EC_{50} (μM)[a]				CC_{50} (μM)[b]
			DENV-1	DENV-2	DENV-3	DENV-4	
huh-7	0.3	Luteolin	7.2±1.07				45.89±2.02
		NITD008	0.54±0.04				~100
		Luteolin		5.19±1.23			45.89±2.02
		NITD008		0.16±0.08			~100
		Luteolin			5.4±1.51		45.89±2.02
		NITD008			0.28±0.07		~100
		Luteolin				8.38±2.10	45.89±2.02
		NITD008				0.11±0.07	~100
HEK-293T	1	Luteolin		12.26±2.30			38.89±1.09
		NITD008		0.12±0.01			~100
A549	0.3	Luteolin		39.16±4.05			93.64±3.09
		NITD008		0.11±0.01			~100
BHK-21	0.3	Luteolin		14.04±3.08			34.73±2.01
		NITD008		0.06±0.02			~100
Vero	0.3	Luteolin		9.36±2.05			~100
		NITD008		0.04±0.004			~100
PBMC	10	Luteolin	15.61±2.07				50.38±3.08
		NITD008	0.46±0.07				~100

[a]Viral titer was determined by plaque assay. EC_{50}s (average 50% effective concentrations) are presented as the mean ± standard deviation from two independent experiments.

[b]Cell viability was measured using CellTiterGlo® Luminescent cell viability Assay. CC_{50}s (50% cytotoxic concentration) are presented as the mean ± standard deviation from two independent experiments. NITD008 was used as the positive control.

Luteolin inhibition of both host and virus protease restricts DENV replication

Fig.1

A.

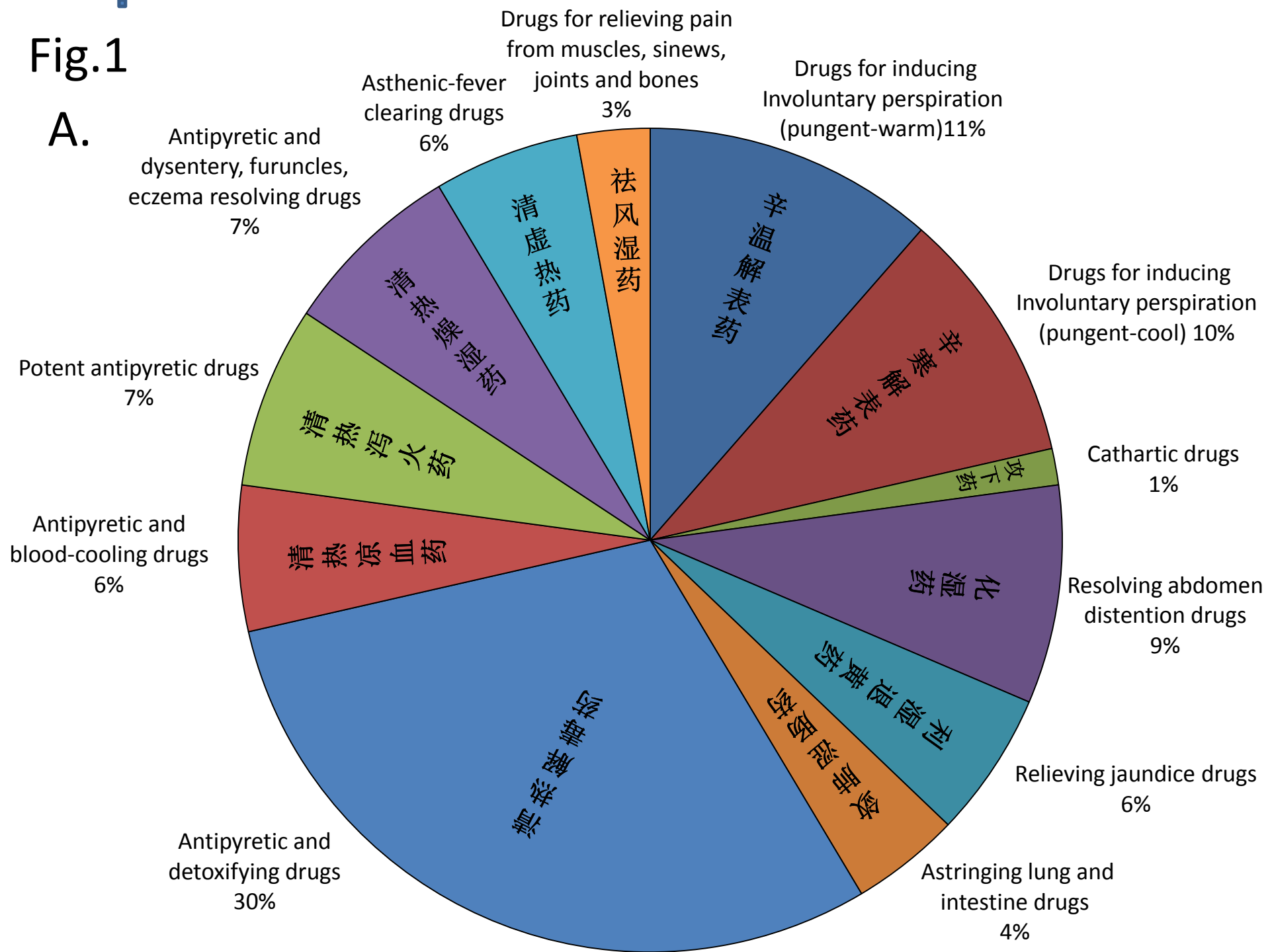
Drugs for relieving pain from muscles, sinews, joints and bones 3%
Asthenic-fever clearing drugs 6%
Antipyretic and dysentery, furuncles, eczema resolving drugs 7%
Drugs for inducing Involuntary perspiration (pungent-warm)11%
Drugs for inducing Involuntary perspiration (pungent-cool) 10%
Cathartic drugs 1%
Resolving abdomen distention drugs 9%
Relieving jaundice drugs 6%
Astringing lung and intestine drugs 4%
Antipyretic and detoxifying drugs 30%
Antipyretic and blood-cooling drugs 6%
Potent antipyretic drugs 7%
祛风湿药
清虚热药
清热燥湿药
辛温解表药
辛寒解表药
攻下药
化滞药
止咳平喘药
收涩固脱药
清热解毒药
清热凉血药
清热泻火药

Fig.1

B.

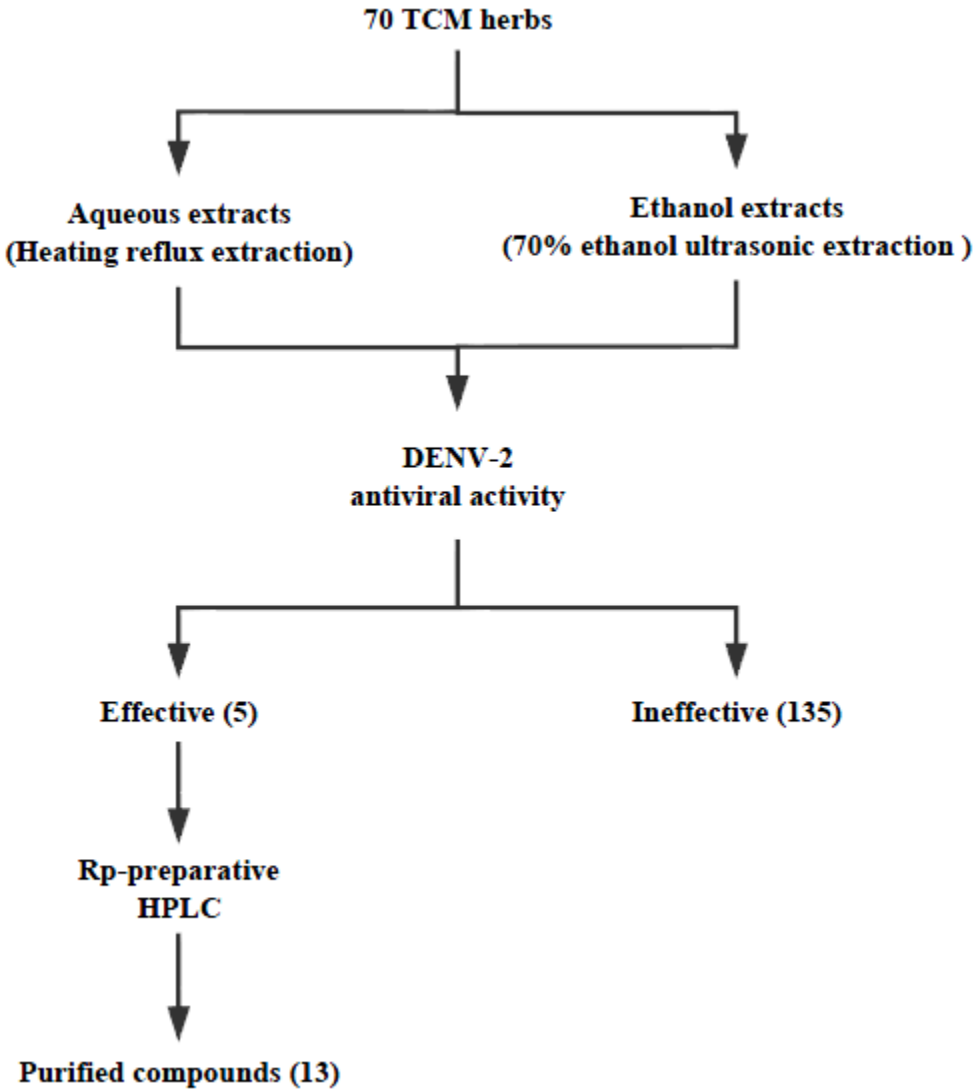
70 TCM herbs
Aqueous extracts
(Heating reflux extraction)
Ethanol extracts
(70% ethanol ultrasonic extraction)
DENV-2
antiviral activity
Effective (5)
Ineffective (135)
Rp-preparative
HPLC
Purified compounds (13)

Fig.1

C.

Paeonia suffruticosa Andr.

Viola yedoensis Makino

Isatis indigotica Fortune.

Lobelia chinensis Lour.

Picrorhiza scrophulariiflora Pennell.

Fig.2

A.

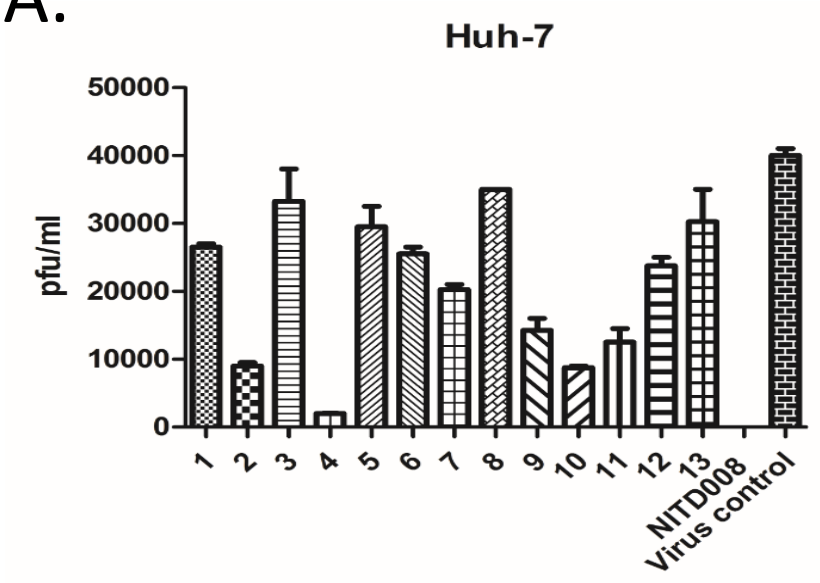
Huh-7
pfu/ml
50000
40000
30000
20000
10000
0
1
2
3
4
5
6
7
8
9
10
11
12
13
NITD008
Virus control

B.

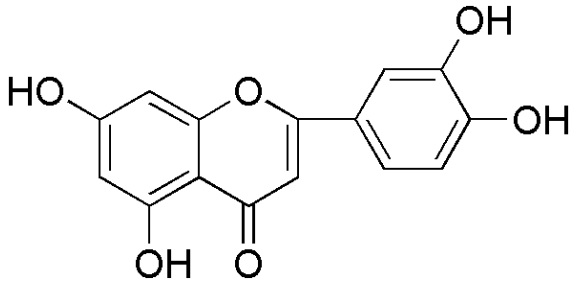
HO
O
OH
OH
OH
O

Table 1

NO.	Chemical name	Structure	Reduction (fold)			
			Huh-7	BHK-21	A549	HEK-293T
1	Quercetin	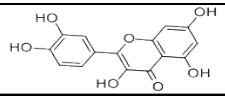	1.51	1.23	0.40	2.02
2	Indirubin	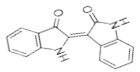	4.44	1.76	1.18	1.95
3	Rutin	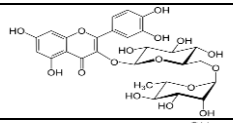	1.20	0.87	0.56	1.32
4	luteolin	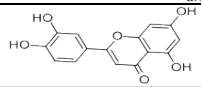	20.02	1.18	0.99	2.43
5	Picroside II	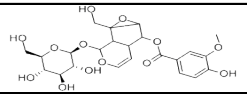	1.36	1.09	0.87	1.92
6	Scopoletin	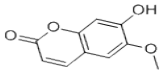	1.57	1.04	2.78	2.33
7	Emodin	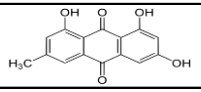	1.98	1.34	0.55	1.65
8	Cinnamic acid	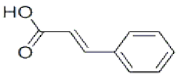	1.14	1.56	0.84	1.19
9	Apigenin	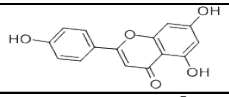	2.81	1.19	0.78	1.89
10	Ursolic acid	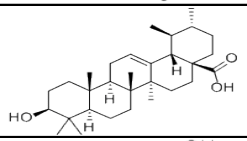	4.57	1.13	7.76	14.17
11	Esculetin	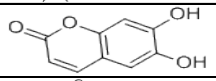	3.20	1.41	0.56	1.72
12	Cichoric acid	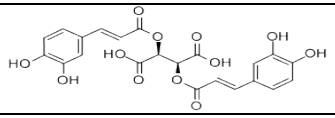	1.68	1.70	1.42	1.47
13	Paeonol	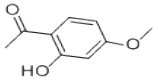	1.32	1.16	0.83	1.45
14	NITD008	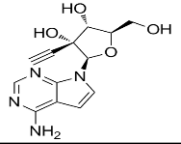	Very high	Very high	17.31	Very high

Fig. 3

A.

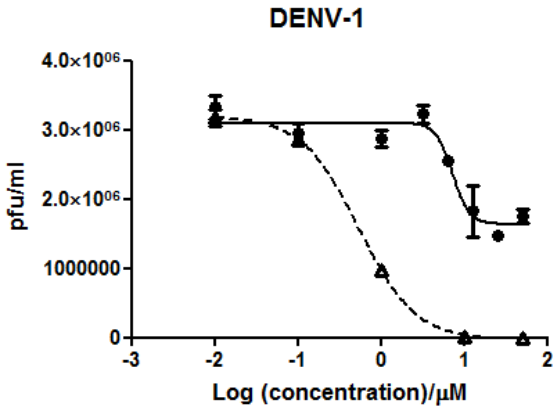
DENV-1
4.0×10^06
3.0×10^06
2.0×10^06
1000000
0
pfu/ml
-3
-2
-1
0
1
2
Log (concentration)/μM

B.

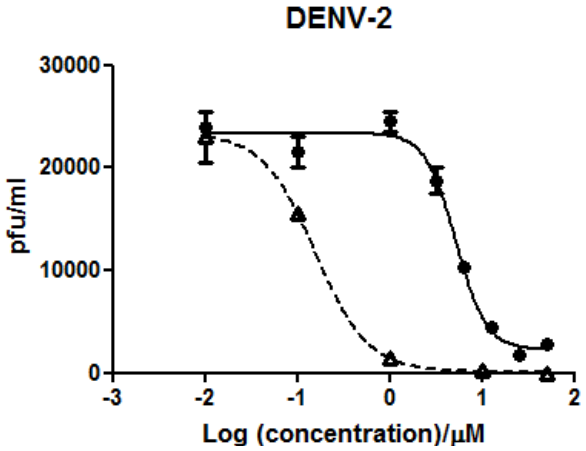
DENV-2
30000
20000
10000
0
pfu/ml
-3
-2
-1
0
1
2
Log (concentration)/μM

C.

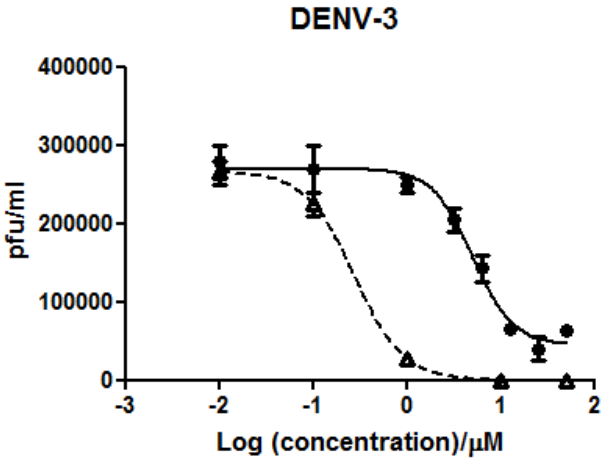
DENV-3
400000
300000
200000
100000
0
pfu/ml
-3
-2
-1
0
1
2
Log (concentration)/μM

D.

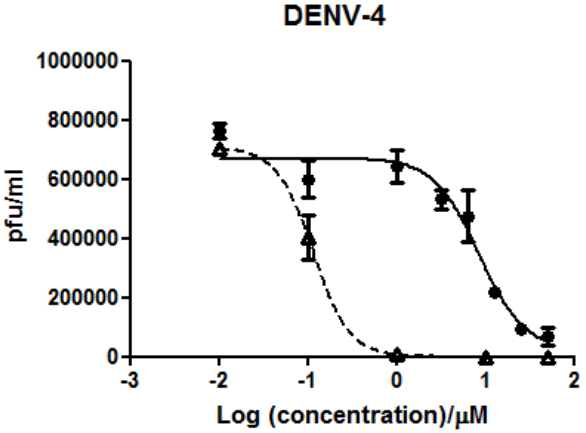
DENV-4
1000000
800000
600000
400000
200000
0
pfu/ml
-3
-2
-1
0
1
2
Log (concentration)/μM

E.

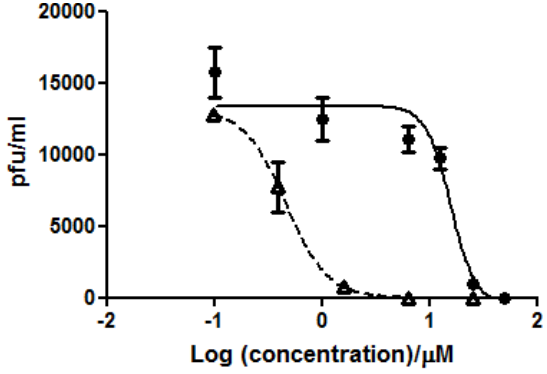
20000
15000
10000
5000
0
pfu/ml
-2
-1
0
1
2
Log (concentration)/μM

Table 2

		EC50				CC50	SI
		DENV-1	DENV-2	DENV-3	DENV-4		
huh-7	Luteolin	7.2				45.89	6.37
	NITD008	0.54				~100	~100
	Luteolin		5.19			45.89	8.84
	NITD008		0.16			~100	~100
	Luteolin			5.69		45.89	8.07
	NITD008			0.28		~100	~100
	Luteolin				8.38	45.89	5.48
	NITD008				0.11	~100	~100
HEK-293T	Luteolin		12.26			38.89	3.17
	NITD008		0.12			~100	~100
A549	Luteolin		39.16			93.64	2.39
	NITD008		0.11			~100	~100
BHK-21	Luteolin		14.04			34.73	2.47
	NITD008		0.06			~100	~100
Vero	Luteolin		9.361			~100	~10.68
	NITD008		0.04			~100	~100
PBMC	Luteolin	15.61				50.38	3.23
	NITD008	0.46				100	~100

Fig.4

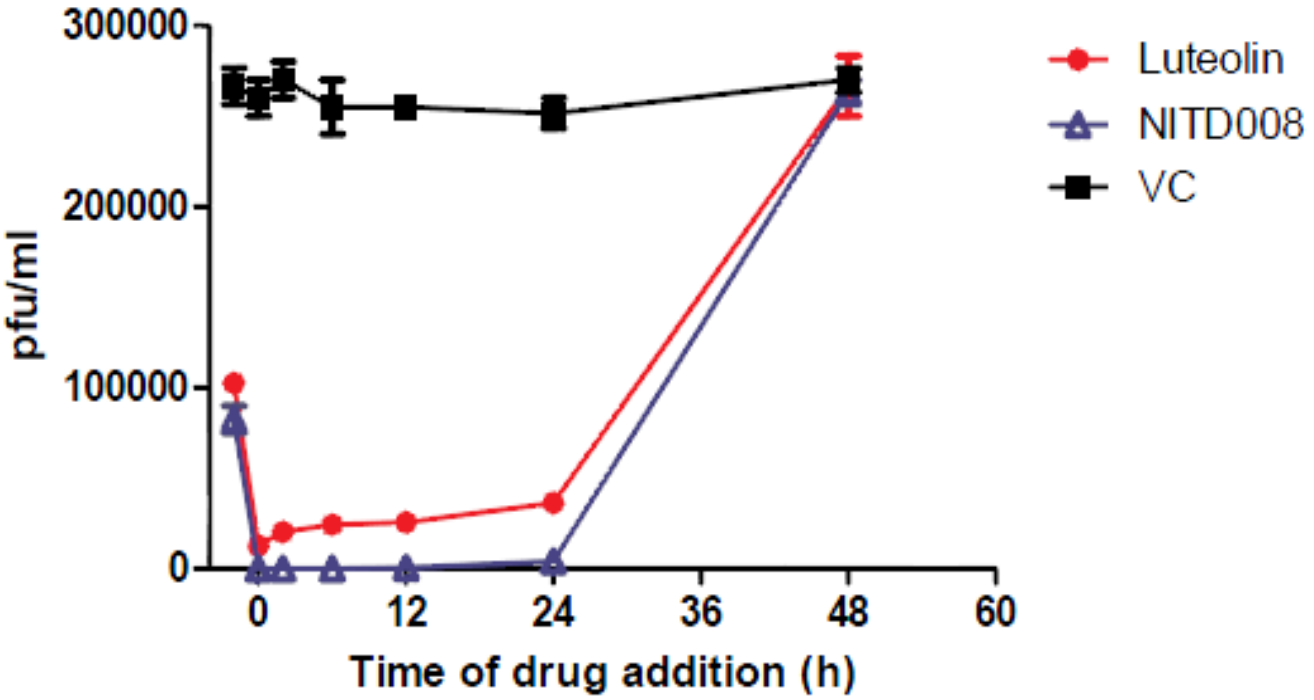
300000
200000
100000
0
pfu/ml
0
12
24
36
48
60
Time of drug addition (h)
Luteolin
NITD008
VC

Fig.5

A.

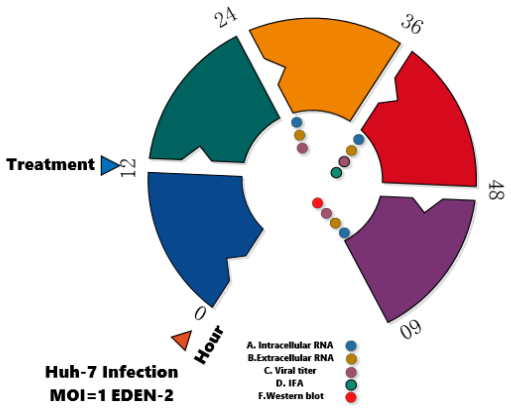
24
36
Treatment
12
48
0
60
Hour
Huh-7 Infection
MOI=1 EDEN-2
A. Intracellular RNA
B.Extracellular RNA
C. Viral titer
D. IFA
F.Western blot

B.

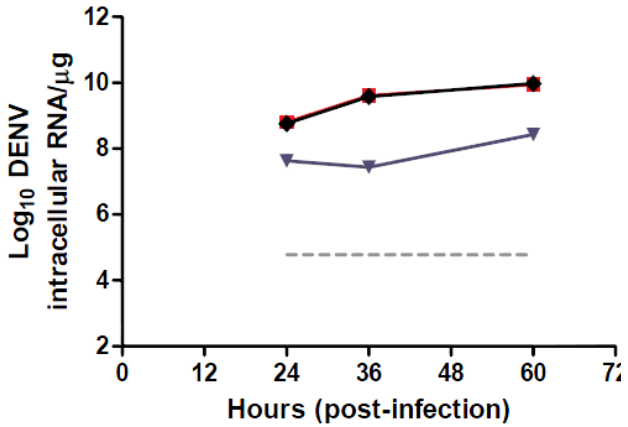
Log10 DENV intracellular RNA/μg
12
10
8
6
4
2
0
12
24
36
48
60
72
Hours (post-infection)

C.

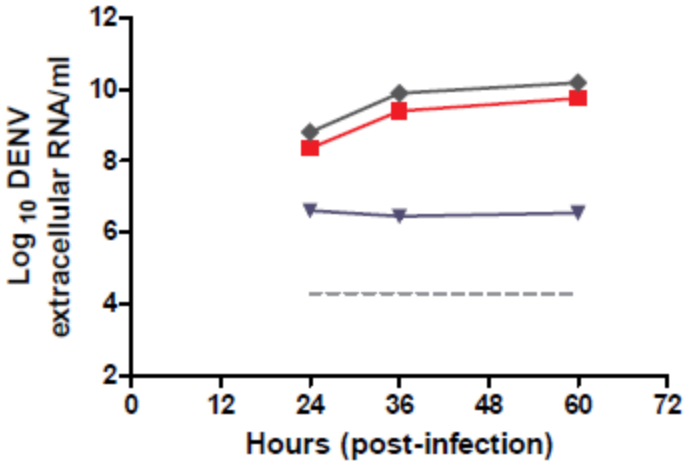
Log 10 DENV extracellular RNA/ml
12
10
8
6
4
2
0
12
24
36
48
60
72
Hours (post-infection)

D.

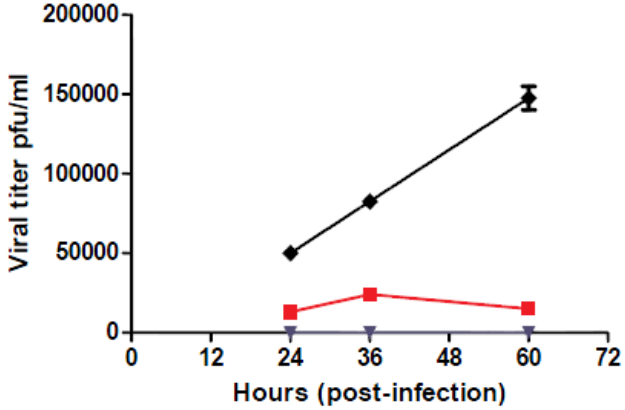
Viral titer pfu/ml
200000
150000
100000
50000
0
0
12
24
36
48
60
72
Hours (post-infection)

E.

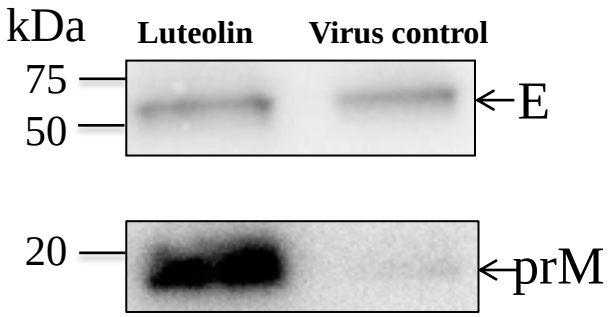
kDa
Luteolin
Virus control
75
50
E
20
prM

Fig.6

A.

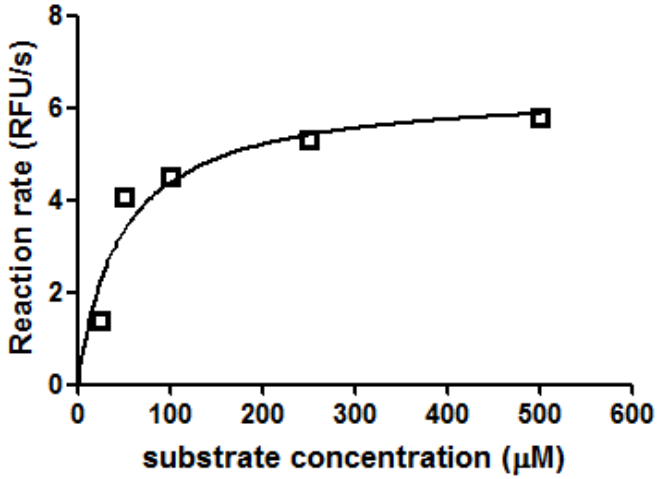
Reaction rate (RFU/s)
substrate concentration (μM)

B.

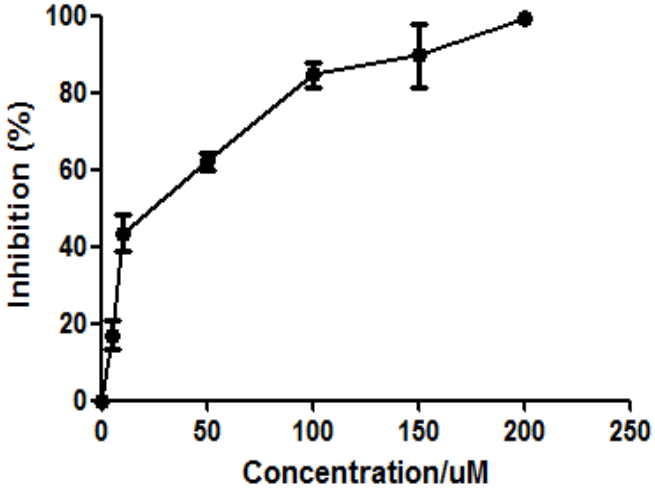
Inhibition (%)
Concentration/uM

C.

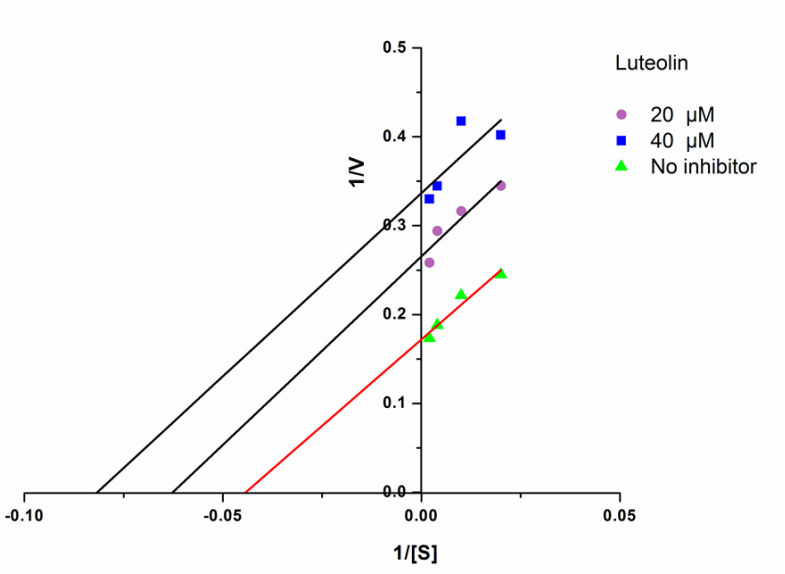
1/V
1/[S]
Luteolin
20 μM
40 μM
No inhibitor

D.

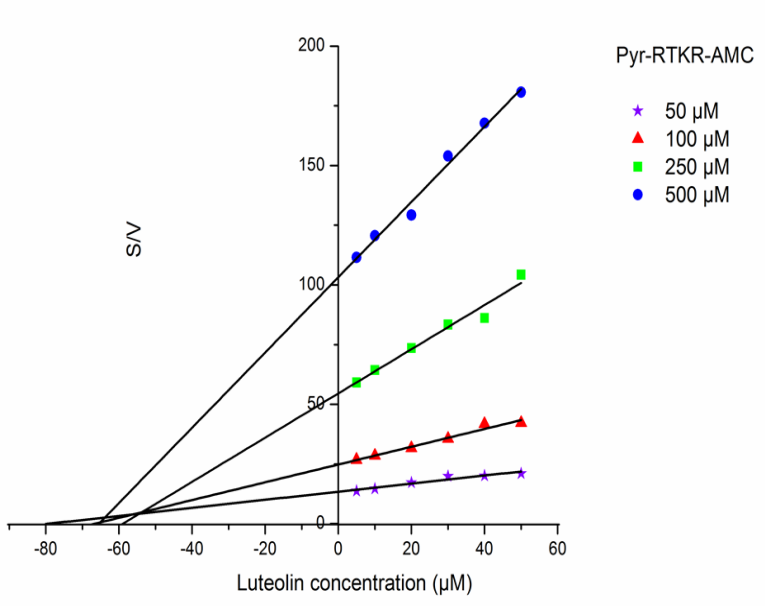
S/V
Luteolin concentration (μM)
Pyr-RTKR-AMC
50 μM
100 μM
250 μM
500 μM

Fig.7

A.

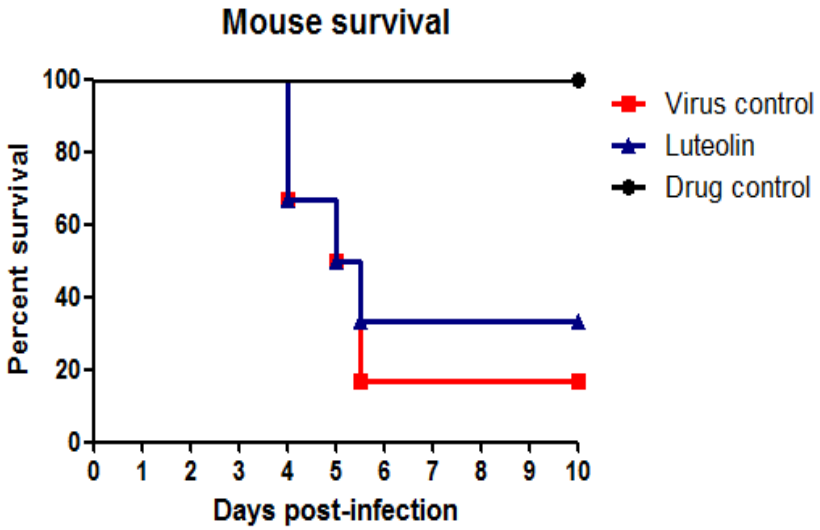
Mouse survival
Percent survival
100
80
60
40
20
0
0 1 2 3 4 5 6 7 8 9 10
Days post-infection
Virus control
Luteolin
Drug control

B.

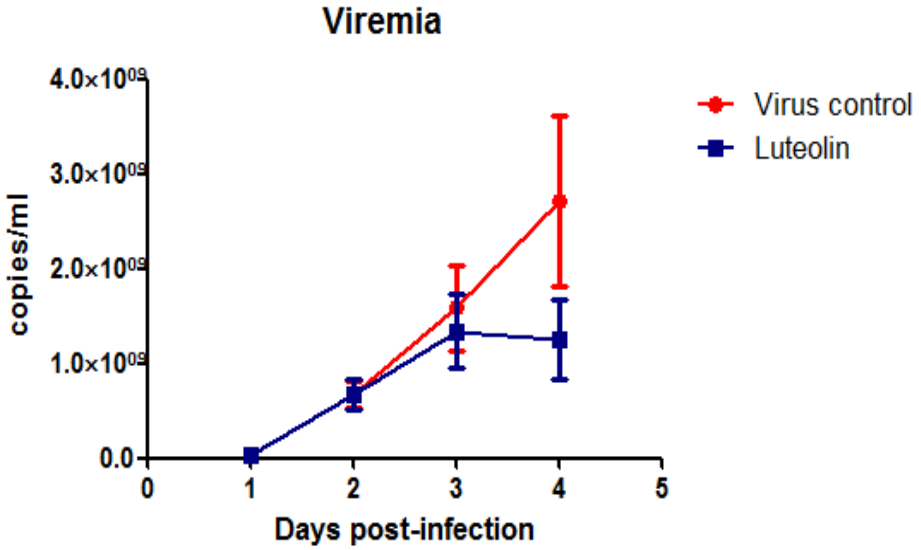
Viremia
copies/ml
4.0×10^09
3.0×10^09
2.0×10^09
1.0×10^09
0.0
0 1 2 3 4 5
Days post-infection
Virus control
Luteolin

C.

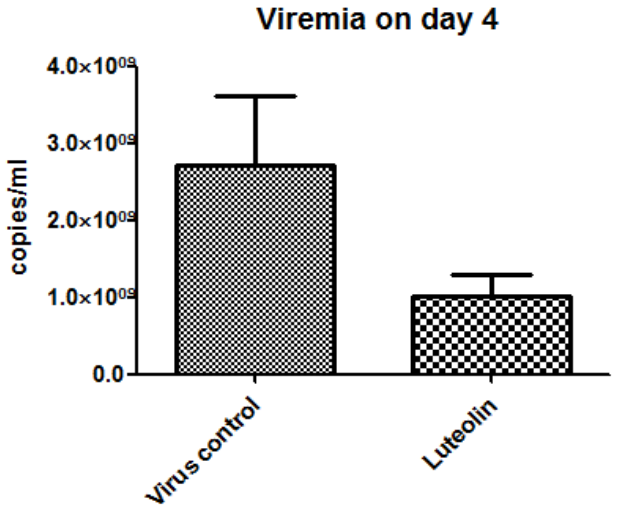
Viremia on day 4
copies/ml
4.0×10^09
3.0×10^09
2.0×10^09
1.0×10^09
0.0
Virus control
Luteolin

Fig.S1A

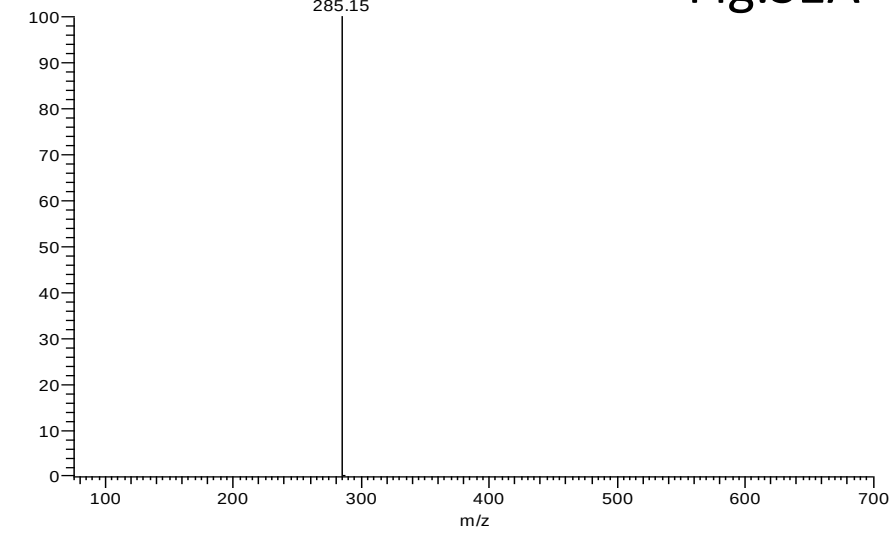

Fig.S1B

	Parameter	Value
1	Title	HQY-C313
2	Comment	
3	Origin	Bruker BioSpin GmbH
4	Owner	nmr
5	Site	
6	Spectrometer	spect
7	Author	
8	Solvent	MeOD
9	Temperature	297.9
10	Pulse Sequence	zgpg30
11	Number of Scans	1024
12	Receiver Gain	188
13	Relaxation Delay	2.0000
14	Pulse Width	10.0000
15	Acquisition Time	1.3631
16	Acquisition Date	2016-09-29T18:31:49
17	Modification Date	2016-09-29T18:31:50
18	Spectrometer Frequency	100.62
19	Spectral Width	24038.5
20	Lowest Frequency	-1957.2
21	Nucleus	13C
22	Acquired Size	32768
23	Spectral Size	65536

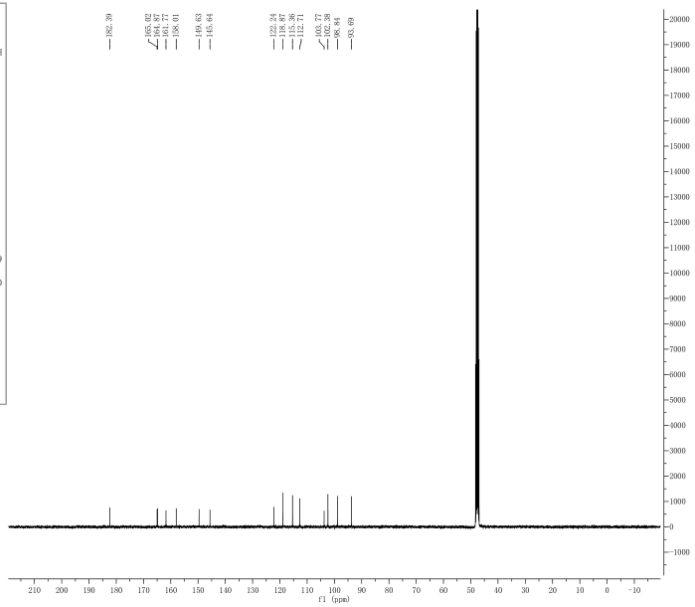

Fig.S1C

	Parameter	Value
1	Title	HQY-C313
2	Comment	
3	Origin	Bruker BioSpin GmbH
4	Owner	nmr
5	Site	
6	Spectrometer	spect
7	Author	
8	Solvent	MeOD
9	Temperature	297.1
10	Pulse Sequence	zg30
11	Number of Scans	16
12	Receiver Gain	107
13	Relaxation Delay	1.0000
14	Pulse Width	10.0000
15	Acquisition Time	4.0894
16	Acquisition Date	2016-09-29T16:39:53
17	Modification Date	2016-09-29T16:39:54
18	Spectrometer Frequency	400.16
19	Spectral Width	8012.8
20	Lowest Frequency	-1582.4
21	Nucleus	1H
22	Acquired Size	32768
23	Spectral Size	65536

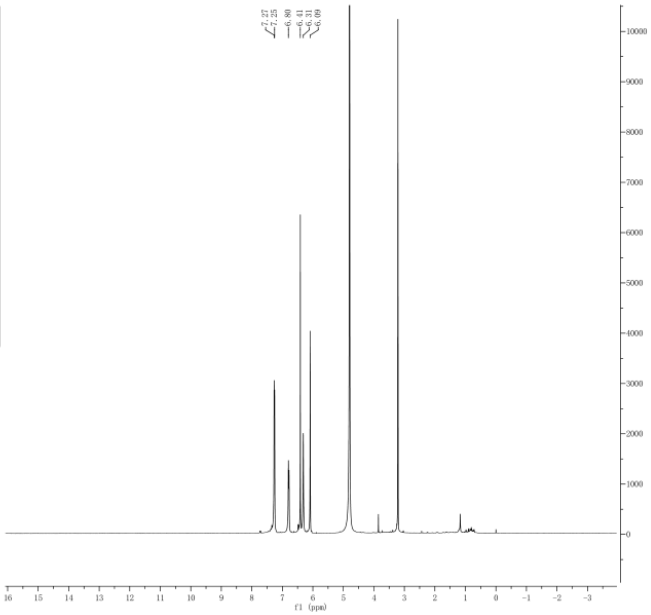

Fig.S2A

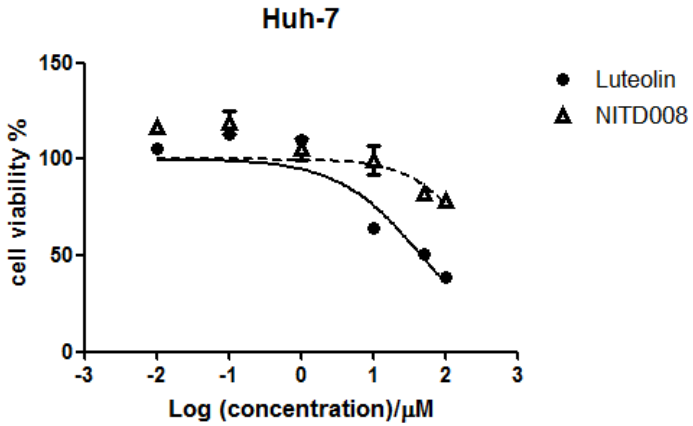

Fig.S2B

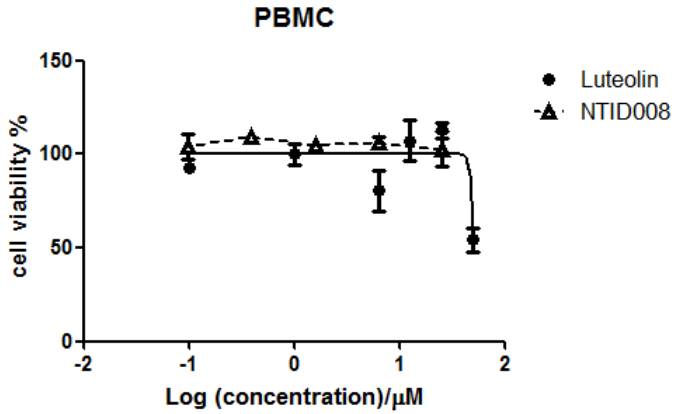

Fig.S3

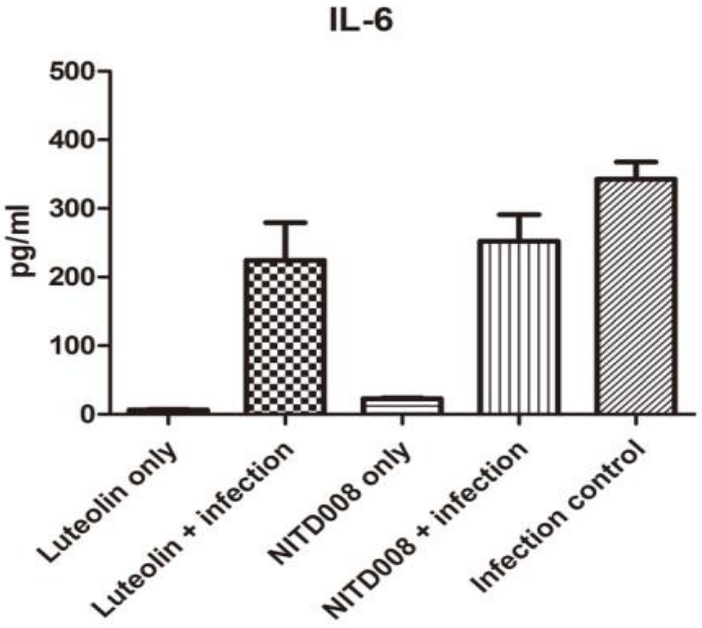
IL-6
pg/ml
500
400
300
200
100
0
Luteolin only
Luteolin + infection
NITD008 only
NITD008 + infection
Infection control

Fig.S4A

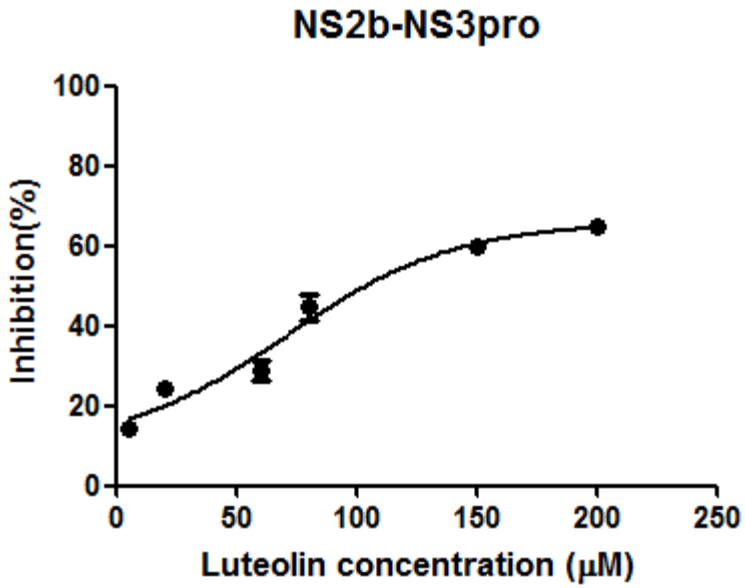

Fig.S4B

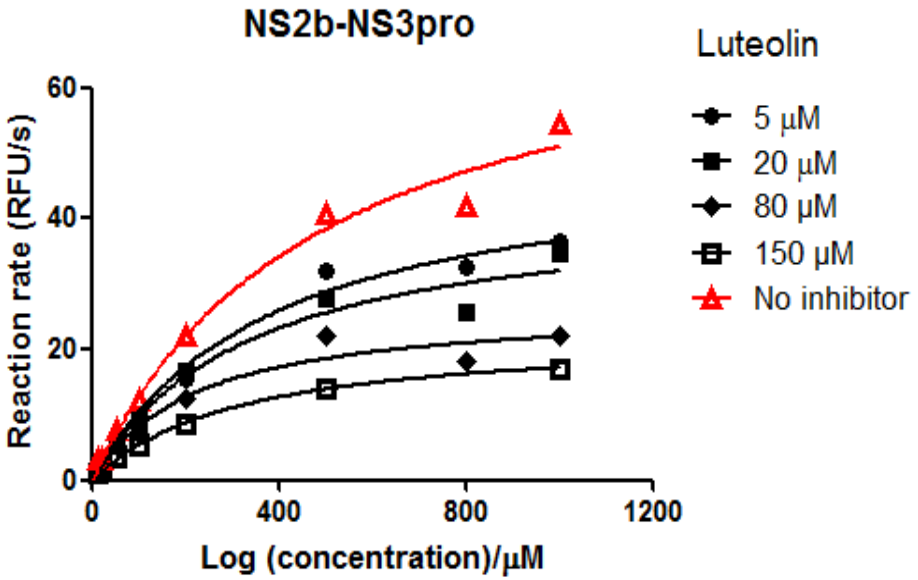

Fig.S4C

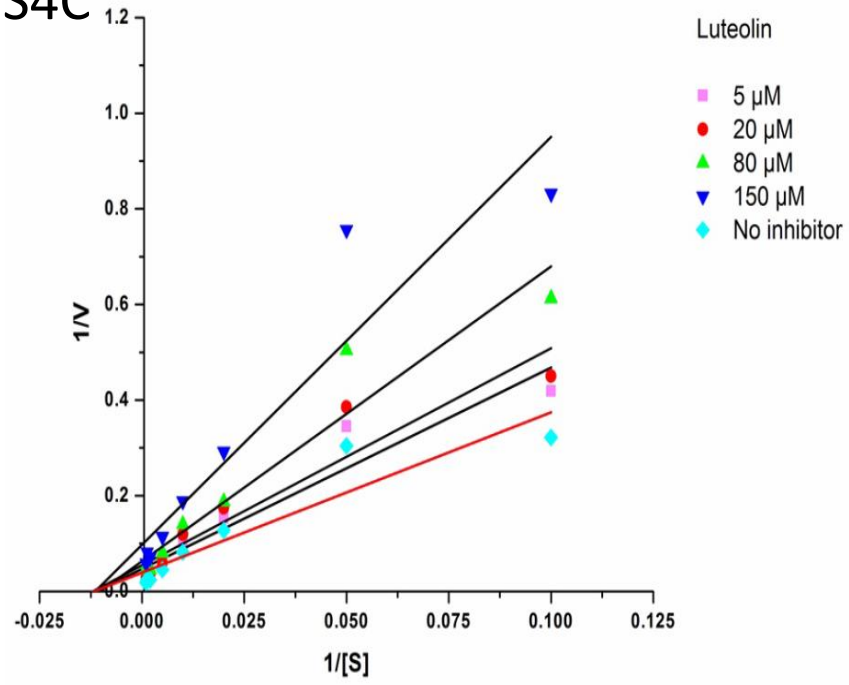

Fig.S4D